Review Article

BIOMEDICAL
Journal of Scientific & Technical Research

ISSN: 2574 -1241

DOI: 10.26717/BJSTR.2020.25.004187

New Insights About Aromaticity using Molecular Polarization, Molecular Quantum Similarity and Chemical Reactivity Descriptors Supported in the Density Functional Theory

Alejandro Morales Bayuelo*

Basic and Clinical Research Group of the Universidad del Sinú, Universidad del Sinú, School of Medicine, Cartagena de Indias, Colombia

***Corresponding author:** Alejandro Morales Bayuelo, Basic and Clinical Research Group of the Universidad del Sinú, Universidad del Sinú, School of Medicine, Cartagena de Indias, Colombia

ARTICLE INFO

Received: January 25, 2020

Published: February 05, 2020

Citation: Alejandro Morales Bayuelo. New Insights About Aromaticity using Molecular Polarization, Molecular Quantum Similarity and Chemical Reactivity Descriptors Supported in the Density Functional Theory. Biomed J Sci & Tech Res 25(2)-2020. BJSTR. MS.ID.004187.

Keywords: Extended Hückel Method; Molecular Polarization; Molecular Quantum Similarity; Chemical Reactivity Descriptores; Density Functional Theory

ABSTRACT

In this work, an extended Hückel method using molecular polarization and quantum similarity is revised, within the Density Functional Theory (DFT) framework. In this extended Hückel method is related the Hückel method and molecular polarization to study Phospho-cyclopentadiene (P-cyclopentadiene), pyrrole, pentalene, thiophene and furan, all with respect to the cyclopentadienyl molecule. In addition, the charges separation is carried out considering a particular set of conjugated diene systems. Expressing the molecular polarizabilities of diene systems as a function of cyclopentadienyl in an external electric field, using the Local Quantum Similarity Index (LQSI) based on the Hirschfeld partitioning and other six local similarity indexes: Overlap, Overlap-Interaction, Coulomb, Coulomb-Interaction, Overlap-Euclidian distance and Coulomb-Euclidian distance.

The molecular alignment is crucial on the quantum similarity, for this reason the Topo-Geometrical Superposition Algorithm (TGSA) is used, which allows us to obtain reliable results. This method can be considered as a straightforward procedure to deal with the problem of relative molecular orientation when we apply Molecular Quantum Similarity (MQS) and represents a new technique that allow us to study structural systems that differ only in one atom. The methodologies revised can be used for future studies on a broader range of systems in which the Hückel method and molecular polarization can be approximated in this form.

With the aim to investigate the stability of the extended Hückel method revised the Diels-Alder reaction are used, the local electrophilicity and hardness are in good agreement with the experimental mechanism of cycloaddition. Additionally, overlap chemical potential and Coulomb potential here proposed reproduce the Fukui function (FF) values trend for dihydrofuran derivatives. Then, in this review new perspectives were postulated in the field of chemical reactivity which allows us to relate the local reactivity indexes with global descriptors. Finally, this review provides new mathematical schemes for the Hückel method considering molecular polarization and quantum similarity under the DFT framework.

Abbreviations: ASA: Atomic Shell Approximation; COMFA: Comparative Molecular Similarity Indexes Analysis; COMSIA: Comparative Molecular Field Analysis; DA: Diels-Alder; DFT: Density Functional Theory; FF: Fukui Function; FMO: Frontier Molecular Orbital; HOMO: Highest Occupied Molecular Orbital; IMPD: Induced Molecular Polarizability Descriptor; LQSI: Local Quantum Similarity Index ; LQS: Local Quantum Similarity; LUMO: Lowest Unoccupied Molecular Orbital; LCAO-MO: Lineal Combination Atomic Orbital-Molecular Orbital ; SALCs: Linear combinations of atomic orbitals adapted to the symmetry; MOB: Masked o-benzoquinone; MQS: Molecular Quantum Similarity;

MQSI: Molecular Quantum Similarity Index; MQSM: Molecular Quantum Similarity Measure; MQSLA: Molecular Quantum Similarity Local Atomic; PCM: Polarizable Continuum Model; PES: Potential Energy Surfaces; PASA: Promolecular Atomic Shell Approximation; QS: Quantum Similarity; QSSA: Quantum Similarity Superposition Algorithm; TGSA: Topo-Geometrical Superposition Approach; TST: Transition State Theory; WH: Woodward-Hoffmann

Introduction

In this work, with the aim to extend the Hückel method on heterocyclic systems, the description of atomic interactions involving molecular polarization and quantum similarity is explored on the Diels-Alder cycloaddition reactions.

Hückel Method and molecular Polarization

Nowadays ab initio calculations are successfully applied in the study of several problems of chemical interest [1-3], which enables us to more efficient and low-cost computational studies. In this context, the Hückel approximation seems appropriate for the study of π conjugated systems, as it provides us theoretical results in good agreement with experimental data [4-9]. In this regard, it is possible to perform molecular electronic calculations in terms of elementary Hückel theory using polarizability [10-16]. Then, in this Computational review we apply the Hückel method to relate a group of chemical molecules with similar structural features, in order to obtain for them, characteristic non-degenerate energy values. Particularly, here we use Molecular Quantum Similarity (MQS), molecular polarizability and the Hückel method, to relate compounds, such as furan, Phospho-Cyclopentadiene (P-Cyclopentadiene) and thiophene (all of point group C2v) with the Cyclopentadienyl (point group D5h), which is used as reference for this application. We propose a local similarity index based on the Hirschfeld partitioning technique [17] to evaluate (dis)similarities at the atomic level.

In line with the increasing importance of quantum techniques in the study of molecular properties and reactions, the indexes based in quantum similarity have received great attention. One of them, known as Molecular Quantum Similarity Index (MQSI), proposed by Carbó and co-workers [18-25], is applied in this research to study the Diels-Alder cycloaddition reaction. In order to study the molecular polarization, the Cyclopentadienyl C–C bond is evaluated as an independent moiety, allowing us to focus on the C–X bonds (where X is the heteroatom). The main idea is to design a theoretical method to relate the induced polarizability for both moieties through some similarity descriptors: the descriptor of overlap and overlap-interaction, that quantify the structural similarity; the descriptor of Coulomb and coulomb-interaction; that quantify the electrostatic similarity between the charge densities of the molecules; and the Overlap and Coulomb Euclidean distances [26-33]. Nowadays nearly all quantum chemical calculations of molecular electronic structure and related properties are studied by ab initio methods [1-5]. These calculations can be successfully applied to predict properties for several chemical systems. However, the interpretation of the results it is not an easy task. In this context, the Hückel method looks as a good option for conjugated-electron systems [31-33] despite the apparent simplicity of this approximation [34-38].

Hückel Method and Molecular Quantum Similarity in Reactions Involving Π-Conjugated Systems

Pericyclic reactions represent an important class of concerted (single step) processes involving π-systems. The fact that reactions are concerted gives us a stereochemical control of the product generation. We suggest that Hückel method can be applied on the pericyclic reactions known as Diels-Alder (DA) processes, where a topological model to quantify the global reactivity indexes is suitable. The DA reaction was discovered some decades ago, and a large number of experimental and theoretical studies have been developed in this regard to understand the mechanism associated with this process [39-41], such as organic Frontier Molecular Orbital (FMO) theory [42], Transition State Theory (TST) [43-45] and more recently static reactivity indexes defined under DFT [46]. Additionally, several topological analyses have been used to determine the mechanism and regioselectivity in such reactions [47-50].

A decade ago, Domingo and Aural studied the chemical reaction between masked o-benzoquinones and furan derivatives [51,52] (2, 4 and 6), see reactions a, b, c; Scheme 1). They suggest that the reaction pathway can be a polar stepwise mechanism. In order to support this statement, we propose a methodology to quantify the global reactivity indexes related with this process, in term of local indexes. This topological analysis is carried out according with the mechanism characteristics proposed in reference [51]. In this research, attention is focus on the theoretical approach based on Quantum Similarity (QS) [12-17] and (DFT) based on reactivity descriptors [6,7], in order to acquire deeper insights into the main factors which govern the nature of cycloaddition reactions. The use of DFT calculations is justified by their accuracy on large systems, low computational cost and theoretical tools they provide us under the so-called conceptual DFT [6,7]. This last point is developed using descriptors such as: electronic chemical potential (μ), electrophilicity (ω) hardness (η) electronegativity (χ) and softness (S). They have been used separately in other studies to understand chemical reactivity and molecular selectivity [2]. In this contribution the main descriptors are hardness, electrophilicity and chemical potential at the global level. A detailed discussion of these quantities can be found on reference [53]. The local property developed in this Computational Review is the Fukui Function (FF), which describes the electron density in a frontier orbital with a slight change in the total number of electrons [54,55].

Molecular similarity indexes allow us to quantify the quantum likeness of two electronic densities [12-17]. Similarity concept is a universal notion that covers almost every field of chemistry. The idea of similarity can be naturally extended to other scientific fields, where a comparison of a property among a set of molecular structures is required. It is important to mention that there is not an absolute value of similarity. We obtain only relative measurements [12-16]. The present computational review is based on similarity indexes computed from molecular fields using the Carbó approach [12-17]. In the quantum similarity the electron density surrounding each molecule is the most important quantity to acquire deeper knowledge about the DA reactions.

Theoretical and Computational Details

Of quantum chemistry methods applied to the study of unsaturated organic molecules, the Hückel method is the most popular. The success of this method is due to its simplicity, which allows even do calculations by hand, when the number of atoms is small and is the simplest method of approximation of molecular orbital theory for unsaturated plane systems additionally is based on the σ-π separation. This method was proposed by Erich Hückel in 1930 and is a very simple Linear Combination of Atomic Orbitals to yield Molecular Orbitals (LCAO MO) method for the determination of energies of molecular orbitals of π-electrons in conjugated hydrocarbon systems, such as ethene, butadiene, benzene and cyclopentadiene among others [55 (a,b)] and was used to test the Woodward–Hoffmann (WH) rules [55(c)]. Initially, it was used for systems with only carbon atoms; however, was later expanded to conjugated molecules such as pyridine, pyrrole and furan that contain atoms other than carbon [55 d)] with some limitations about the electronic correlation or the structural geometry.

The Hückel method can be used for determining the molecular orbitals, but it is not very successful in determining the structural geometry of an organic molecule due to that the electron-electron repulsions are not explicitly included and the total energy is just a sum of terms for each electron in the molecule, also this method works poorly for molecules that contain atoms of very different electronegativity [55(e)]. For this reason, in this review is presented a new mathematic scheme on the Hückel method using molecular polarization and quantum similarity in the (DFT) context, in order to find new parameters to improve the use of Hückel method in organic physicochemical [55 (f)].

Molecular Polarization in An External Electric Field as A Parameter to Correct The Hückel Method

In this research, with the aim to obtain the molecular description of the polarization in heterocyclic systems as the P-cyclopentadiene is proposed the application of the molecular polarization of two identical atoms under an external electric field which can be the (C1-C2) bond in the cyclopentadienyl and proposed by Kovalenko et al. [56(a)]. Suppose that the electrons can do transitions of the form 2s 3p. All possible initial states of the system under study are described by wave functions.

$$\Psi_m^L = \sum_{\mu} s_{L,\mu,m-\mu}^{(l,\bar{l})} \Psi_{\mu} \bar{\Psi}_{m-\mu}$$

Where $s_{L,\mu,m-\mu}^{(l,\bar{l})}$, are the Wigner coefficients [56(b)]

nd the over barred symbols refer to the states of the second atom. Using the relation (1) can be determined the 16 initial states of the system of atoms, see **Appendix Figure 1**.

Linearly Polarizad Field: Under the action of an electric field **E = (E$_1$i +E$_2$j+E$_3$k)cos(ωθ)**. The quantum states of this system can be given by the equation:

$$i\hbar\frac{\partial}{\partial t}\Psi = \left(\hat{\mathbf{H}}_0 + \hat{\bar{\mathbf{H}}}_0 + \hat{\mathbf{V}}\right)\Psi \qquad (2)$$

with

$$\Psi = \sum_{k=1}^{16} a_k \Psi_k \exp(-i\omega_k t) \qquad (3)$$

$$\omega_k = \begin{cases} 2\omega_1, k = 1 \\ \omega_1 + \omega_2, k = \overline{2,7} \\ 2\omega_2, k = \overline{8,16} \end{cases} \qquad (4)$$

Where $\hbar\omega_1$ and $\hbar\omega_2$ are the energies of the 2s and 3p, $\hat{H}_0$ and $\hat{\bar{H}}_0$ represent the Hamiltonians of the atoms, and $\hat{V} = -(D,E)$, $D = d + \bar{d}$, $d + \bar{d}$ are the operators of the dipole moments of the atoms. Equation 3 yields the system of differential equations ($\dot{a}$) of the equation 5.

$$i\hbar\dot{a} = Va \qquad (5)$$

To solve this equation 5, is used the method of successive approximations given in equation 4:

$$a = I - \int_0^t V(\tau)d\tau \qquad (6)$$

(a) denotes a square matrix of order 16 where each column defines the wave function $|\Psi_k\rangle$ of the atoms-plus-field system in the corresponding initial state see **Appendix Table 1**. For calculate the polarization of this system is used the equation 7, therefore for the molecule A we have:

$$\mathbf{P}_{\mathbf{kA}} = Sp\hat{\rho}_k\mathbf{D} \qquad (7)$$

Here $\hat{\rho}_k = |\Psi_k\rangle\langle\Psi_k|$, and the operator (D) is constructed using the basis of functions (equation 1). This allows obtain the expressions for the corresponding initial states (see **Appendix Table 2**). Taking in account the equation 7, is propose the multiplication of this by the similarity descriptors, this new local descriptor can be named *"Induced Molecular Polarizability Descriptor (IMPD)"* and can quantify the (dis)similarity between the molecular polarization and the quantum similarity on the heterocycles studied.

Similarity Indexes as Parameters to Relate Groups of Molecules, using the Hückel Method.

The (MQS) field was introduced by Carbó-Dorca [57-61]. He defined the Euclidean distance, d_{AB}, between the electronic densities $\rho_A(r)$ and $\rho_B(r)$ of two molecules A and B as:

$$d_{AB} = \int \left|\rho_A(r) - \rho_B(r)\right|^2 dr = \int \rho_A^2(r)dr + \int \rho_B^2(r)dr - 2\int \rho_A(r)\rho_B(r)dr \qquad (8)$$

Now this index can be represented geometrically using the concept of cosine of angle subtended between the density functions, considering as vectors. It is written as:

$$R_{AB} = \frac{\int \rho_A(r)\rho_B(r)dr}{\left[\left(\int \rho_A^2(r)dr\right)\left(\int \rho_B^2(r)dr\right)\right]^{1/2}} = \frac{Z_{AB}}{\sqrt{Z_{AA}Z_{BB}}} \qquad (9)$$

This equation involving the overlap integral Z_{AB}, often called Molecular Quantum Similarity Measure (MQSM), between the electronic densities of molecules A and B. Z_{AA} and Z_{BB} are called the Molecular Quantum Self-Similarity Measures of molecules A and B [57].

Local Quantum Similarity índex (LQSI) for the Estructures.

For the conversion of the global Carbó index into a local index was possible using the Hirschfeld portioning [58]. The calculation of Local Quantum Similarity Index (LQSI) with DFT is a very used method [60], considering that the point Group of cyclopentadienyls D_{5h} with P-cyclopentadiene C_{2v} structurally differ only by the presence of a different atom. According to the idea of Hirschfeld, obtaining atoms-in-molecules densities by defining the ''stock-amount'' or weight of an atom **P** in the electronic density at ***r*** as:

$$w_P(r) = \frac{\rho_P^0(r)}{\sum_X \rho_{X,P}^0(r)} \qquad (10)$$

Here, $\rho_P^0(r)$ is the electronic density of the isolated phosphor atom in the molecule, and $\sum_X \rho_{X,P}^0(r)$ is the pro-molecular density of the molecule, obtained as the sum of the isolated atom densities in the same molecular geometry as the actual molecule. The Hirschfeld atomic electronic density of the atom **P** in the molecule denoted can be calculated as:

$$\rho_P(r) = w_P(r)\rho_P(r) \qquad (11)$$

analogously, for the cyclopentadienyl

$$w_C(r) = \frac{\rho_C^0(r)}{\sum_Y \rho_{Y,C}^0(r)} \qquad (12)$$

the numerator of the Carbó index then becomes

$$Z^{local,P} = \int w_P \rho(r)dr = \int \left(\frac{\rho_P^0(r)}{\sum_X \rho_{X,P}^0(r)}\right)\rho_P(r)dr \qquad (13)$$

and, for the cyclopentadienyl

$$Z^{local,C} = \int w_C \rho(r)dr = \int \left(\frac{\rho_C^0(r)}{\sum_Y \rho_{Y,C}^0(r)}\right)\rho_C(r)dr \qquad (14)$$

Whereas the self-similarities $Z_{PP} = \left(Z^{local,P}\right)^2$ and $Z_{CC} = \left(Z^{local,C}\right)^2$ can be written analogously in terms of atomic contributions, using the equations (13 and 14) in the expression of the Carbó index (equation 9) and the global index is converted into a local analogue:

$$R_{PC}^{local} = \frac{Z^{local,P}Z^{local,C}}{\sqrt{\left(Z^{local,P}\right)^2\left(Z^{local,C}\right)^2}} = \frac{\int \left(\frac{\rho_P^0(r)}{\sum_X \rho_{X,P}^0(r)}\right)\left(\frac{\rho_C^0(r)}{\sum_Y \rho_{Y,C}^0(r)}\right)\rho_P(r)\rho_C(r)dr}{\left[\int \left(\frac{\rho_P^0(r)}{\sum_X \rho_{X,P}^0(r)}\right)^2 \rho_P(r)\rho_P(r)dr\right]^{1/2}\left[\int \left(\frac{\rho_C^0(r)}{\sum_Y \rho_{Y,C}^0(r)}\right)^2 \rho_C(r)\rho_C(r)dr\right]^{1/2}} \qquad (15)$$

Where the global index is partitioned in its atomic contributions, this Hirschfeld approach is used taking in account the holographic electron density theorem postulated by Mezey et al. [61]. To circumvent expensive computational calculations, trimolecular Atomic Shell Approximation (**ASA**) has been used routinely to compute density functions and fitted electronic density functions from H to Rn for use in quantum similarity measures. The principal problem with the calculation of Carbó and Hodgkin-Richards index is their dependence with the relative orientation of the molecules. The problem has been addressed through the use several methodologies with criterions such as aligning of the molecules according to common physicochemical features (for example, matching different three-dimensional molecular fields such as steric, electrostatic, or hydrophobic fields) [62, 63] or alignment of the molecules based on topological and geometrical features only, as has been implemented in the methodology called Topo-Geometrical Superposition Algorithm (**TGSA**) [64] this algorithm is based on comparisons of atom types and interatomic length. Other methods are based in the maximizing of the similarity measure [65]. In this framework, a new algorithm, the Quantum Similarity Superposition Algorithm (**QSSA**), was recently designed by Bultinck et al. [65,66], expressing the relative position of two molecules in terms of mutual translation in three cartesian directions and three Euler angles. The quantum similarity overlap, considering the electronic densities of the molecules within the Trimolecular Atomic Shell Approximation (**PASA**) [66] and considering the atomic electron densities within the (**ASA**) [62-75], is then used to optimize the mutual positions and similarity of the molecules, using a Lamarckian genetic algorithm. In this review, we decided to superimpose the common fragment shown in (Figure 1), using the (**TGSA**), considering the rigidity of the rings, as relevant structural criteria [76,77].

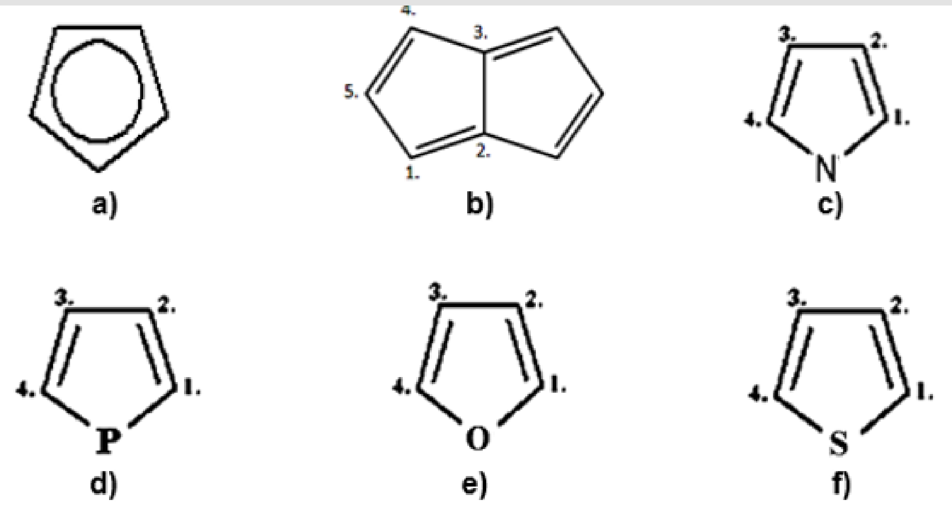

Figure 1:
(a) Structure of the cyclopentadienyl of point group D5h (reference system),
(b) furan,
(c) P-cyclopentadiene and
(d) thiophene all point group (C2v). Its atoms used for superposition are labeled.

All charge densities used in this Computational Review were calculated using the **Gaussian 09** program packages [77] at the **HF/6-31+G(d,p)** [78(a-c)] and **B3LYP/6-31+G(d,p)** levels [78(d-f)] which can be expected to be adequate for the purpose of our study. One of the big advantages of the use of the alignments produced by TGSA is that these alignments have better consistency with the experimental results than with those produced by Maxim or QSSA based on total electron densities and by this reason is used in this research. One of the basic postulates of quantum mechanics applied to chemistry states that for every molecule or state a wave function exist that is all-determining. This means that, once the wave function is known, every so-called observable property for an N-electron molecule may be obtained by straightforward integration as in equation 16:

$$\Omega[\Psi] = \iint \ldots \int \Psi^*(x_1,\ldots,x_N)\hat{\Omega}(x_1,\ldots,x_N)\Psi dx_1 \ldots dx_N \quad (16)$$

Where $(\hat{\Omega})$ is the appropriate operator for that specific observable property. It is worth locating where the electron density is highest in a molecule. It is found that the electron density values are highest in the volumes defined by the sub valence regions of every atom [79]. It is also well known that in those regions, chemical bonding produces only small density changes compared with the isolated atoms, which suggests the possibility of composing an approximate molecular electron density as a sum of isolated atom densities. Taking in account that the molecule formation will change the electron densities from the summed-up atomic electron densities, but we may expect that this will have only a relatively small effect on the (MQSM) values. Moreover, the idea of an approximate electron density composed of superposing isolated atom electron densities organized in the same geometrical way as in the true molecule has a long history [58].

Chemical Reactivity Descriptors

The last application of Hückel theory involves making predictions regarding some chemical reactions we encountered during our study of organic chemistry. Specifically, we will make predictions regarding cycloadditions with electrophilic-nucleophilic interactions. An electrophile is a species in search of electron density. Hückel theory can tell us which carbon atom in a molecule has the most accessible electron density. By accessible, we mean electrons that are of highest energy, and as we know those electrons will be found within the HOMO. Now also we must know that the electrons in an orbital are spread across all of the atoms in the molecule in proportion to the square of the coefficients multiplying their respective atomic orbitals. Therefore, the carbon atoms p orbitals with the largest squared coefficients in the HOMO will be the atoms most likely to undergo the cycloadditions.

On the other hand, the nucleophilic species involves the donation of electron density. That election density will most likely be placed in the empty MO of lowest energy, the LUMO. The carbon atoms with the largest squared coefficients in the LUMO, once again, will be the sites best able to accept the donated electron density and will therefore be the sites of cycloaddition. In the DFT context [80,81]. The electron density is calculated as:6

$$\rho_A = \sum_{\upsilon\mu} D_{\upsilon\mu}\varphi_v\varphi_\mu^* \quad (17)$$

Where (D) represents the charge and the binding order of the matrix and (φ_v) are the basis functions used in the iterative process of the Self Consistent Field (SCF). In this context the similarity measurements are obtained by the expression:

$$Z_{AB} = \sum_{v\in A}\sum_{\mu\in A}\sum_{\delta\in B}\sum_{\lambda\in B} D_{v\mu}D_{\delta\lambda}\int \varphi_\mu^*(r)\varphi_v(r)\varphi_\lambda^*\varphi_\delta(r)dr \quad (18)$$

To calculate the integral in equation 18 is used the classical approach of overlapping of Gaussian type orbitals. In this study is related the electron density with the call shape function ($\sigma_A(r)$) according to Parr et al. [82], this can be obtained by the relation:

$$\sigma_A(r) = N_A^{-1}\rho_A(r) \qquad (19)$$

Where N_A is the number of electrons in the molecule A. The shape function determines each observable of the system and may give information about the number of electrons in the electron density, despite that is Minkowski normalized to unit in all molecules:

$$\int \sigma_A(r)dr = 1 \qquad (20)$$

To use this shape function, we considered the relationship with several indexes as was demonstrated by Bultinck and coworkers [83,84]. Using this type of mathematical consideration from the point of view of the behavior of the electronic density, we can calculate the total energy and the similarity indexes. In the chemical reactivity framework, the total energy can be obtained through the use of the expression:

$$E_{v_0}[\rho] = F[\rho] + \int \rho(r)\upsilon_0(r)dr \qquad (21)$$

Where (F) represents the original function of Hohenberg-Kohn theorem provided by the sum of the kinetic energy (T) and the functional energy electron-electron repulsion (Vee) [85,86]. The variation of first order in the total energy is:

$$dE[N,\upsilon_0(r)] = \left(\frac{\partial E}{\partial N}\right)_{\upsilon_0(r)} dN + \int\left(\frac{\delta E}{\delta\upsilon_0(r)}\right)_N \delta\upsilon_0(r)dr \qquad (22)$$

from equation 21 we have

$$\left(\frac{\delta E}{\delta\upsilon_0(r)}\right)_N = \rho(r) \qquad (23)$$

using equation 22 it is possible to define the chemical potential, through the relationship.

$$\mu \equiv \left(\frac{\partial E}{\partial N}\right)_{v_0(r)} \qquad (24)$$

substituting equations 23 and 24 into equation 20 it is obtained the relationship:

$$dE[N,v_0(r)] = \mu dN + \int \rho(r)\delta\upsilon_0(r)dr \qquad (25)$$

The chemical potential (μ) can be interpreted as the measurement of the tendency of electrons to escape from the electron cloud, whose discontinuity for integer values, of N was shown by Perdew et al. [87], the second term equation 25 is called Hellmann-Feynman term [88]. From chemical reactivity point of view, the first and second derivatives are important. It is considered the second order change in energy with respect to the number of electrons and the external potential through variations in the chemical potential:

$$d\mu[N,\upsilon_0(r)] = \left(\frac{\partial\mu}{\partial N}\right)_{\upsilon_0(r)} dN + \int\left(\frac{\delta\mu}{\delta\upsilon_0(r)}\right)_N \delta\upsilon_0(r)dr \qquad (26)$$

and electron density:

$$\delta\rho[N,\upsilon_0(r);r] = \left(\frac{\partial\rho(r)}{\partial N}\right)_{\upsilon_0(r)} dN + \int\left(\frac{\delta\rho(r)}{\delta\upsilon_0(r)}\right)_N \delta\upsilon_0(r)dr \qquad (27)$$

In equation 26 the first term relates to the chemical hardness (η), expressed mathematically as:

$$\eta \equiv \left(\frac{\partial\mu}{\partial N}\right)_{\upsilon_0(r)} = \left(\frac{\partial^2 E}{\partial N^2}\right)_{\upsilon_0(r)} \qquad (28)$$

The equation 28 can quantify the opposition that puts the system to deform its electron cloud [88], while the second term in equation 26 represents the term called linear response function ζ(r,r´) [88].

Using the Maxwell relations in equation 22 is possible define the Fukui functions [89] and equation 23 and 24:

$$f(r) \equiv \left(\frac{\partial\rho(r)}{\partial N}\right)_{\upsilon_0(r)} = \left(\frac{\delta\mu}{\delta\upsilon_0(r)}\right)_N \qquad (29)$$

using equations 28 and 29, is obtained for the equations 26 and 27:

$$d\mu[N,\upsilon_0(r)] = \eta dN + \int f(r)\delta\upsilon_0(r)dr \qquad (30)$$

$$\delta\rho[N,\upsilon_0(r);r] = f(r)dN + \int w(r,r')\delta\upsilon_0(r)dr \qquad (31)$$

Interpreting the Fukui functions ($f(\vec{r})$) from equations 30 and 31, we can explain the bond formation between two molecules A and B. In first instance, we consider the case where the chemical potential of reagent A is higher than the reagent B, in this case the similarity from the point of view of overlapping in the electronic distribution (equation 18) is low, increasing the fit between the electron densities of A with respect to B. Now consider the case of the electronic overlap between molecule A and B when the electron density $\rho_A(r)$ tends to increase the number of electrons, N_A:

$$f_A^+(r) \equiv \left(\frac{\partial\rho_A(r)}{\partial N_A}\right)^+_{\upsilon_{0,A}(r)} = \lim_{\varepsilon\to 0}\left[\frac{\rho[N+\varepsilon,\upsilon_0(r)] - \rho[N,\upsilon_0(r)]}{2\varepsilon}\right] \qquad (32)$$

This implies that (FF^+) is large in regions where there is high susceptibility to attack by nucleophilic species. Now consider the case of the electronic density B versus electron density A having few electrons.

$$f_B^-(r) \equiv \left(\frac{\partial\rho_B(r)}{\partial N_B}\right)^-_{\upsilon_{0,B}(r)} = \lim_{\varepsilon\to 0}\left[\frac{\rho[N,\upsilon_0(r)] - \rho[N-\varepsilon,\upsilon_0(r)]}{2\varepsilon}\right] \qquad (33)$$

From which we can conclude that the molecule B donates electrons in regions where (FF^-) is large. Finally, we consider the case when the variations of electrons are $(\Delta N_A \approx \Delta N_B \approx 0)$ using the concept of lateral boundaries, as:

$$f^0(r) \equiv \lim_{\varepsilon\to 0}\frac{\rho[N+\varepsilon,\upsilon_0(r)] - \rho[N-\varepsilon,\upsilon_0(r)]}{2\varepsilon} \qquad (34)$$

$$= \frac{f^+(r) + f^-(r)}{2} \qquad (35)$$

From where we can get the following relations:

$$I = A,B : f_I^0(r) \equiv \frac{f_I^+(r) + f_I^-(r)}{2} \qquad (36)$$

These expressions can be used to predict reactivity sites in neutral or radical species. In this regard, these reactivity descriptors were used in this dissertation for carry out the aims proposed with the guiding review.

Results and Discussion

Considering the aims was developed a review about the extended Hückel method proposed by the present author using molecular polarization and quantum similarity on heterocycles and dimmer systems as pentalene. Finally, with the aim to evaluate the extended Hückel method proposed is development a topological study using chemical reactivity descriptors in Diels-Alder reactions.

Extended Hückel Method Using Molecular Polarization and Quantum Similarity Estudies Proposed.

In order to describe the electronic similarity of heterocyclic systems in this study reported in the reference [25], the Hückel method to P-cyclopentadiene, as a function of cyclopentadienyl (Figure 1) is expressed, instead of taking into account the interactions of phosphor with the neighboring carbon atoms and this methodology is applied to all the heterocycles studied taking to cyclopentadienyl as reference. We are proposing the introduction of local similarity index of the Phosphor atom in P-cyclopentadiene with respect to the carbon of cyclopentadienyl in the construction of the secular determinant. Using n time the i-th reducible representation occurs in an irreducible representation (Γ_π= E= 5, C_2= -1, σ_v(xz)= -5, σ_v(yz)= 1) where we know only the characters of each representation by the equation 37, (see **Appendix Table 3**).

$$a_i = \frac{1}{h}\sum_R \chi(R)\chi_i(R) \qquad (37)$$

Where (h) represents the order of the group. We find the secular determinant of the linear combinations of atomic orbitals adapted to the symmetry (SALCs).

$$\begin{vmatrix} H_{11}-E & H_{12} & . & . & 0 \\ H_{12} & H_{22}-E & . & . & 0 \\ . & . & H_{33}-E & H_{34} & H_{35} \\ . & . & H_{43} & H_{44}-E & H_{45} \\ 0 & 0 & H_{53} & H_{54} & H_{55}-E \end{vmatrix} = 0 \qquad (38)$$

Applying Hückel approximations. We have:

$$H_{11} = \int \psi_1 H \psi_1 d\tau = \alpha, H_{12} = \int \psi_1 H \psi_2 d\tau = \beta, H_{22} = \int \psi_2 H \psi_2 d\tau = \alpha - \beta, H_{33} = \int \psi_3 H \psi_3 d\tau = I^s\alpha,$$

$$H_{34} = \int \psi_3 H \psi_4 d\tau = \sqrt{2}\beta, H_{35} = \int \psi_3 H \psi_5 d\tau = 0, H_{44} = \int \psi_4 H \psi_4 d\tau = \alpha, H_{45} = \int \psi_4 H \psi_5 d\tau = \beta,$$

$$H_{55} = \int \psi_5 H \psi_5 d\tau = \alpha + \beta$$

Where (I^S) in () represents the proposed local quantum similarity of the P-cyclopentadiene phosphor atom with respect to the carbon atom of the cyclopentadienyl, therefore the two components secular determinant is $\begin{vmatrix} \alpha - E & \beta \\ \beta & \alpha - \beta - E \end{vmatrix} = 0$, whose solutions represent the energies associated with the dimension $A_2(E_1 = \alpha - 1.618\beta,\ E_2 = \alpha + 0.618\beta)$, similarly for the other determinant, taking into account that the difference between the P-cyclopentadiene and the cyclopentadienyl is the presence of phosphor, we intend to introduce the local similarity index Overlap, Coulomb with their Euclidean distances, specifically in the integral ( ) in the secular determinant, resulting

$$\begin{vmatrix} I^s\alpha - E & \sqrt{2}\beta & 0 \\ \sqrt{2}\beta & \alpha - E & \beta \\ 0 & \beta & \alpha + \beta - E \end{vmatrix} = 0 \qquad (39)$$

These determinants will allow us to express the application of the method Hückel in the P-cyclopentadiene (point group C_{2v}) in function of the application of the method applied in the cyclopentadienyl of symmetry D_{5h}.

The first descriptor will use the local similarity index of overlap, which will allow us to quantify the structural similarity between the phosphor atom and carbon atom of the cyclopentadienyl, with their euclidean distance, when decrease the Euclidean distance indicates that the structures are structurally very similar; due to that the structures differ only by a single atom, we associate these lengths with the local structural similarity of overlap between the two atoms, in (Table 1) is shows the values of the six indexes of (MQS).

In (Table 1) we can see a local similarity index of Overlap 0.964 and of Coulomb 0.996, this allows say that the effects associated with the structure as bond distance, atomic size and hybridization sp2 of the atom phosphor with respect to the some hybridization of atom carbon in the cyclopentadienyl of symmetry D5h, are more appreciable that the electronic effects as the location of the resonant system (Figure 2), and presence of an additional electron in the P-cyclopentadiene with respect to the cyclopentadienyl, such results can be checked with their euclidean distances that for the local similarity index Overlap is 0.461 and for the local similarity index Coulomb is 1.426. (Figure 3) shows the chemical behavior of P-cyclopentadiene in the electronic distribution indicated by the respective resonance structures (Figure 2), such behavior is associated with a low acid character due a that the phosphorus and carbon atoms are protonated and the resonant system is very stable, it details shows opposition to donate a hydrogen atom according to with the chemical formalism of Bronsted-Lowry theory, (Figure 3).

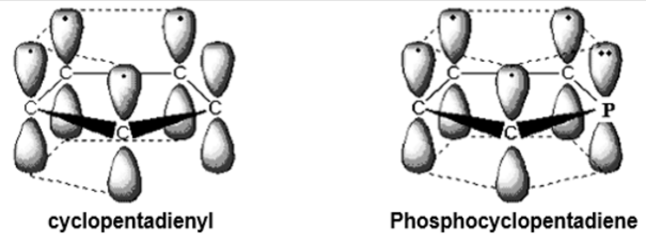

Figure 2: Comparison of the resonant system of cyclopentadienyl with respect to the P-cyclopentadiene.

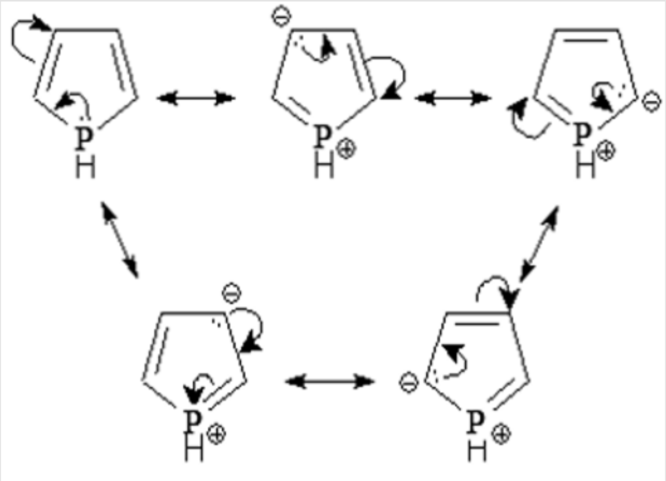

Figure 3: Resonance structures of P-cyclopentadiene.

Table 1: Local Similarity Index (Analytical and Numerical Method) and euclídea distance, using global densities for the P-cyclopentadiene vs cyclopentadienyl [25].

Structure	$Z_{CP}(O)^{c}$	$Z_{CP}(C)^{d}$	$LSI(O)^{e}$	LSI(C)f	DCP(O)g	DCP(C)h
P-cyclopentadiene[a] vs cyclopentadienyl[b]	2.86	188.767	0.964	0.996	0.461	1.426

[a] Point Group C2v

[b] Point Group D5h

[c] Interaction of Overlap

[d] Interaction of Coulomb

[e] Local Similarity Index of Overlap

[f] Local Similarity Index of Coulomb

[g] Euclidean Distance of Overlap

[h] Euclidean Distance of Coulomb

In (Figure 4), we can see in contrast the electronic properties for cyclopentadienyl, these having more anionic characteristic in their behavior, according with the rule of (4n + 2 electrons) in the P-cyclopentadiene. Sp^{2} carbon of cyclopentadienyl (quantified by the local MQS index with respect to Overlap of the P-cyclopentadiene), is very acidic because the conjugate base of the cyclopentadienyl anion is aromatic and therefore very stable. In (Table 1) we can see that the euclidean distance of overlap are larger than those of Coulomb, this is because the bond length (C-P) in the P-cyclopentadiene are higher that the of the (C-C) in the cyclopentadienyl (Figure 5), and this is evidenced by the lower local similarity index of Overlap with respect to the Coulomb index. The high values in the local similarity indexes observed in (Table 1), shows that the method TGSA alignment is a method suitable for our purpose, taking into account that the TGSA method considers the molecules as rigid bodies; also it is able to recognize a common substructure, providing a coherent alignment with chemical intuitive sense. In (Figure 5), we can see differences in the length among the carbon-carbon bond in cyclopentadienyl and the phosphor-carbon bond of the P-cyclopentadiene, which give rise to different molecular polarizations. On the other hand, this (Figure 5) shows that the lengths between bonds on the actual structure of cyclopentadienyl compared with those of P-cyclopentadiene are similar, so our initial review does not consider the polarization of the atoms neighboring the site of interest is well justified (Table 1).

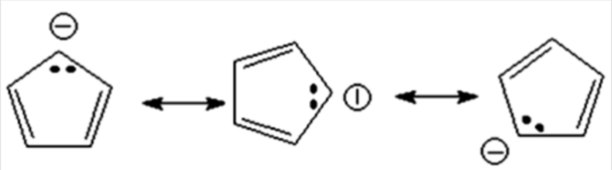

Figure 4: The cyclopentadienyl anion resonance forms are all aromatic, with respect to the electronic behavior of P-cyclopentadiene.

(a) Bond distance of cyclopentadienyl.

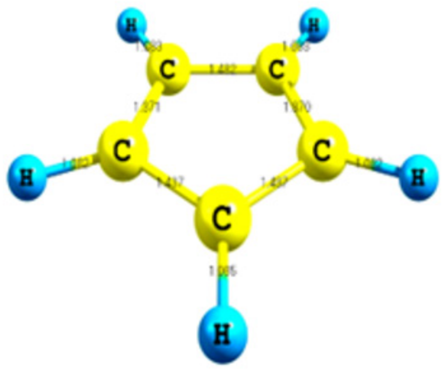

(b) Bond distance of P-cyclopentadiene.

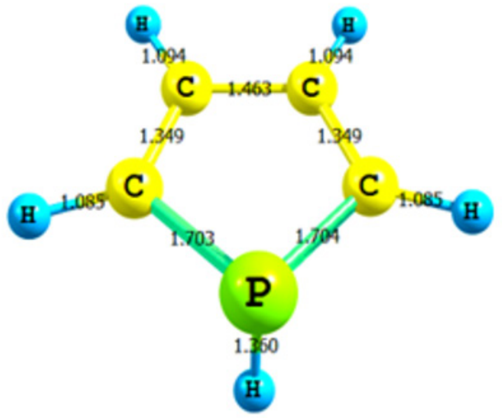

Figure 5: Comparison of the bond length ((Å) Armstrong units) of

(a) cyclopentadienyl and

(b) P-cyclopentadiene [25].

(Figure 6) shows the tendency of the dipole moment and total atomic charges; we see that the trend for the P-cyclopentadiene is oriented toward the phosphor atom, due to the electronegative character (with a total atomic charge of 0.436), which results in the loss symmetry of the molecular orbital, and the probability of finding the electron is greater in the vicinity of the more electronegative atom, unlike in the cyclopentadienyl of orientation toward the center of the ring, this is due to the resonant characteristic (Figure 2) where the asymmetric carbon has a total atomic charge of -0.099, these characteristic for the electric charge in the rings is measured by the Coulomb index (Table 1). In (Table 2) we can observed that the energies of the orbitals of P-cyclopentadiene as a function of the energies of cyclopentadienyl has nondegenerate values, taking into account their local indexes of similarity approximately the unit (Table 1), naturally the Carbó index is limited to the range (0,1), where C_{AB}=1 means self-similarity, according to the Schwartz integral inequality [90,91]:

Table 2: Orbital energies values of P-cyclopentadiene as a function of the orbital energies of cyclopentadienyl, for each Similarity descriptor (Table 1).

Energy Values Reported			
Index	**E_3**	**E_4**	**E_5**
LSI(*O*)[a]	$0.964\alpha + 1.928\beta$	$0.964\alpha + 0.190\beta$	$0.964\alpha + 3.666\beta$
LSI(*C*)[b]	$0.996\alpha + 1.992\beta$	$0.996\alpha + 0.189\beta$	$0.996\alpha + 3.789\beta$
$D_{CP}(O)$[c]	$0.461\alpha + 0.922\beta$	$0.461\alpha + 0.090\beta$	$0.461\alpha + 1.753\beta$

$D_{CP}(C)^{d}$	$1.426\alpha + 2.852\beta$	$1.426\alpha + 0.271\beta$	$1.426\alpha + 5.423\beta$
$i\text{-}(O)^{e}$	$2.860\alpha + 5.720\beta$	$2.8860\alpha + 0.564\beta$	$2.8860\alpha + 0.564\beta$
$i\text{-}(C)^{f}$	$188.767\alpha + 377.534\beta$	$188.767\alpha + 35.865\beta$	$188.767\alpha + 717.843\beta$

[a] Local Similarity Index of Overlap

[b] Local Similarity Index of Coulomb

[c] Euclidean Distance of Overlap

[d] Euclidean Distance of Coulomb

[e] Overlap-Interaction

[f] Coulomb-Interaction

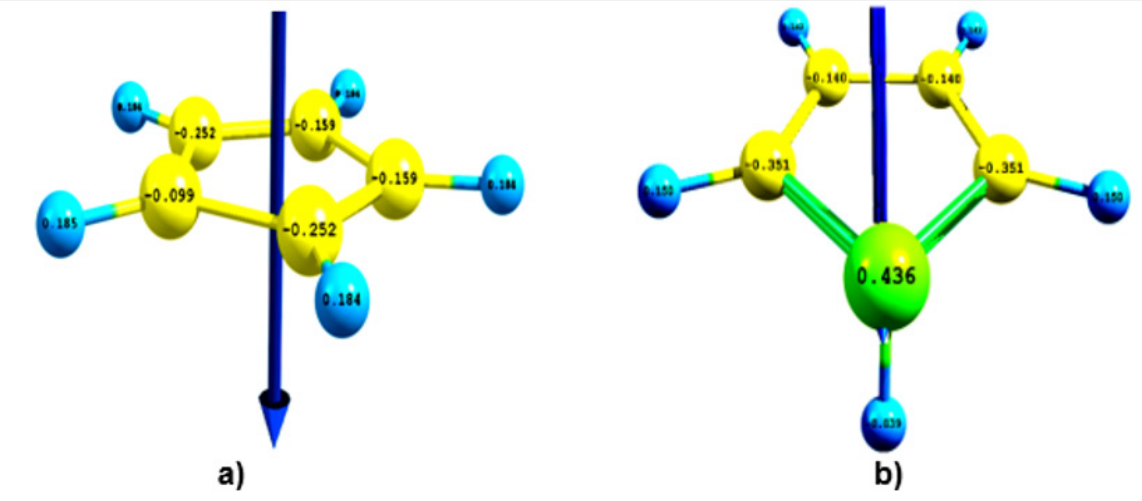

Figure 6:
Dipole moment and total atomic charges:
(a) cyclopentadienyl and
(b) P-cyclopentadiene [25].

$$\left[\int \rho_A(r)\rho_B(r)\,dr\right]^2 \leq \int \rho_A^2(r)\,dr \int \rho_B^2(r)\,dr \qquad (40)$$

When ρ_A and ρ_B are the electronic density.

The results of (Table 2) demonstrate that the quantum similarity is an alternative, which allowed us to break the energy degeneration, providing alternatives to solve the problem of obtaining nondegenerate values in systems where the approximations of the traditional Hückel method provide degenerate values. In (Figure 7) is performed the comparison in the orbital degeneration between cyclopentadienyl and P-cyclopentadiene. In (Table 3) shows the values of the molecular polarizations using the equation 7, which allows quantify the molecular polarization in the (C-P) bond of P-Cyclopentadienyl. These aromatic compounds are characterized from the structural point of view by their molecular plane and have a circular system of delocalized electrons above and below of this molecular plane. This cloud circular comes from the interaction of p orbitals of the atoms in the cycle, sp2 hybridized. In the Hückel approximation the orbital diagrams are represented using the energy levels. The energy diagram of (Figure 7) has the energy levels of the cyclopentadienyl (a) with respect to the energy levels of the P-cyclopentadiene (b) proposed in this study, these energy levels to P-cyclopentadiene shows nondegenerate values and a form to understand the aromaticity in this type of systems consistent with the experimental details.

Table 3: Molecular polarizability descriptors for the P-cyclopentadiene (PB) in function of molecular polarizability of cyclopentadienyl (PA), Proposed in this study.

Induced Molecular Polarizability Index For P_B:					
$2.860P_{nA}^{a,b}$	$188.767P_{nA}^{a,c}$	$0.964P_{nA}^{d}$	$0.996P_{nA}^{e}$	$0.461P_{nA}^{f}$	$1.426P_{nA}^{d}$

Note: n is the quantum states (see appendix 1 and 2).

[a] Analytical Method

[b] Interaction of Overlap

[c] Interaction of Coulomb

[d] Local Similarity Index of Overlap

[e] Local Similarity Index of Coulomb

[f] Euclidean Distance of Overlap

[d] Euclidean Distance of Coulomb

PA: Eq. 7. With respect to the polarizability states.

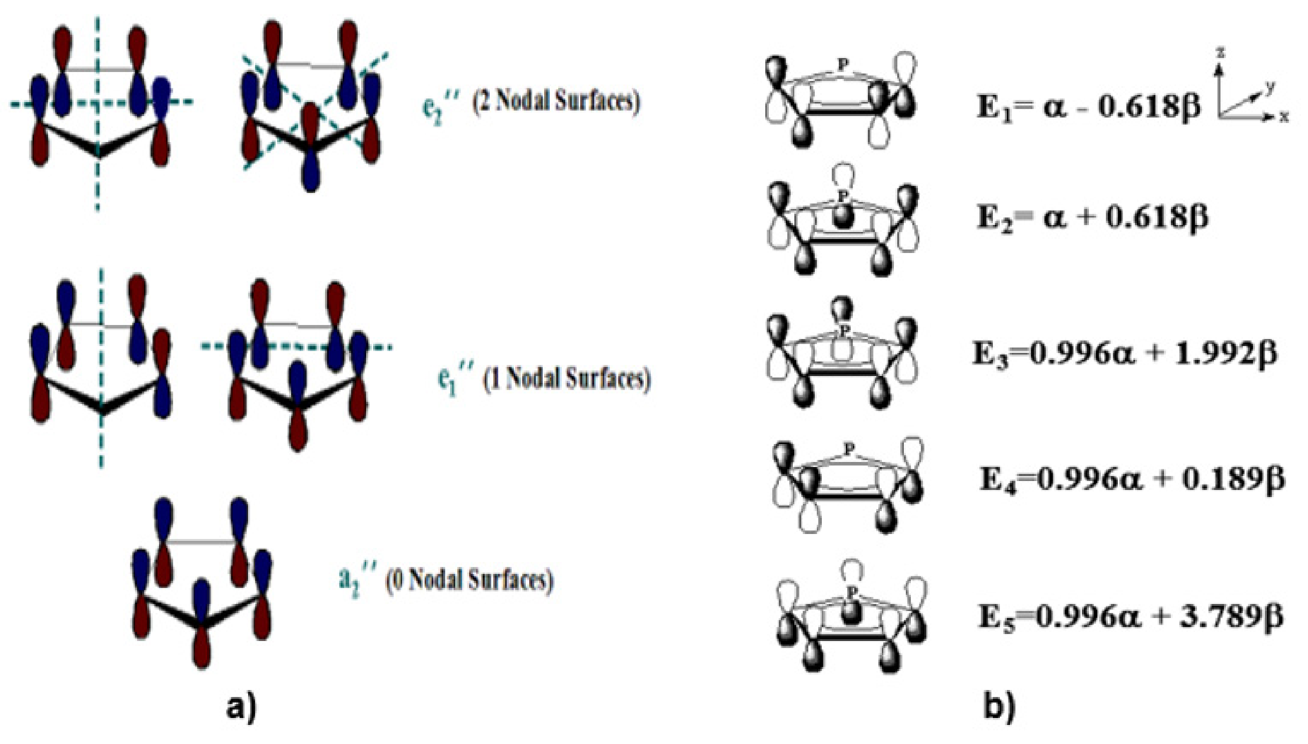

Figure 7:

(a) Orbital degeneration of Hückel method in the cyclopentadienyl,

(b) breaking of the orbital degeneracy in the Hückel method of P-cyclopentadiene, proposed in this study.

Note: In the Figure (b) is used the orbital energy of Coulomb index of Table 2.

where:

$$\mathbf{P_{1B}} = (\mathbf{P_{1A}})\left[SI\right] = (Sp\hat{\rho}_k\mathbf{D})\left[R_{PC}^{local}\right]$$

$$= (Sp\hat{\rho}_k\mathbf{D})\left[\frac{\int\left(\frac{\rho_P^0(r)}{\sum_X \rho_{X,P}^0(r)}\right)\left(\frac{\rho_C^0(r)}{\sum_Y \rho_{Y,C}^0(r)}\right)\rho_S(r)\rho_C(r)dr}{\left[\int\left(\frac{\rho_P^0(r)}{\sum_X \rho_{X,P}^0(r)}\right)^2 \rho_P(r)\rho_P(r)dr\right]^{1/2}\left[\int\left(\frac{\rho_C^0(r)}{\sum_Y \rho_{Y,C}^0(r)}\right)^2 \rho_C(r)\rho_C(r)dr\right]^{1/2}}\right] \quad (41)$$

(Figure 8). IMPD for the P-cyclopentadienyl in an external electric field proposed in this study. Note: P_{1A}: is the equation 7 and R_{PC}^{local}: is the equation 15. This equation 41 includes interactions of the induced dipoles by the atoms, considering that in this model there is not point masses and inelastic collisions. Therefore, these interactions allow asymmetric charge distribution resulting an induced polarization, taking in account the induced dipole moment concept [85]. Additionally, its descriptor (equation 41) can relate different dipole moments depending of the polarizability states (see **Appendix Table 2**). These methodological proposed allow us to find new molecular descriptors of energy and local polarizability in an external electric field, relating local atoms in the structures studied and can be complementary to the reported by Krishtal et al. [92-94], so we can define these new local descriptors as potential descriptors taking into account that is with respect to another molecule that are calculated. It is the main reason to express a system in terms of another according to Morales-Bayuelo et al. [94-96]. The equation 41 shows the analysis of the polarization on the thiophene and furan with respect to cyclopentadienyl, (Figure 9).

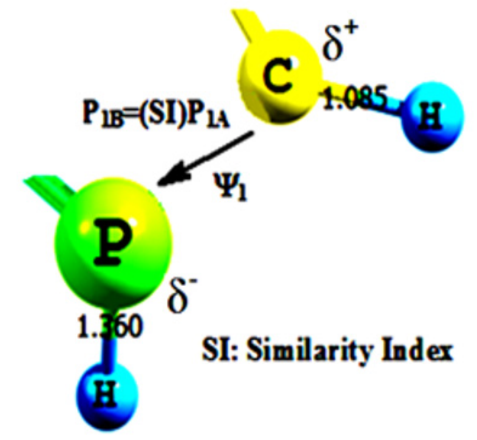

Figure 8: IMPD for the P-cyclopentadienyl in an external electric field proposed in this study.

Note: P1A: is the equation 7 and : is the equation 15.

On the other hand, the electronic effects such as the resonance are more relevant in the thiophene with respect to the furan due to the presence of an additional electron in comparison with cyclopentadienyl. These results were supported by an euclidean distance of overlap of 0.410 and an euclidean distance of coulomb 0.966 to the thiophene, an euclidean distance of overlap of 0.871 and an euclidean distance of coulomb 2.009. All carbon atoms in thiophene and furan are sp^2 hybridized, thus we have four electrons remaining for pi bonding. The sulfur and oxygen atoms have two lone pairs and two bonds (which normally lead to a sp^3 hybridization). In contrast, in a sulphur atom, the electrons of the lone pair are promoted to the p orbital and the hybridization of all the other carbons is produced (three sp^2 and one p) therefore it cannot be considered a (4n + 2) electronic system. On the other hand, in (Figure 9), we can see that the electronic pair over the negatively charged carbon of the cyclopentadienyl anion obeys the (4n + 2) electron rule.

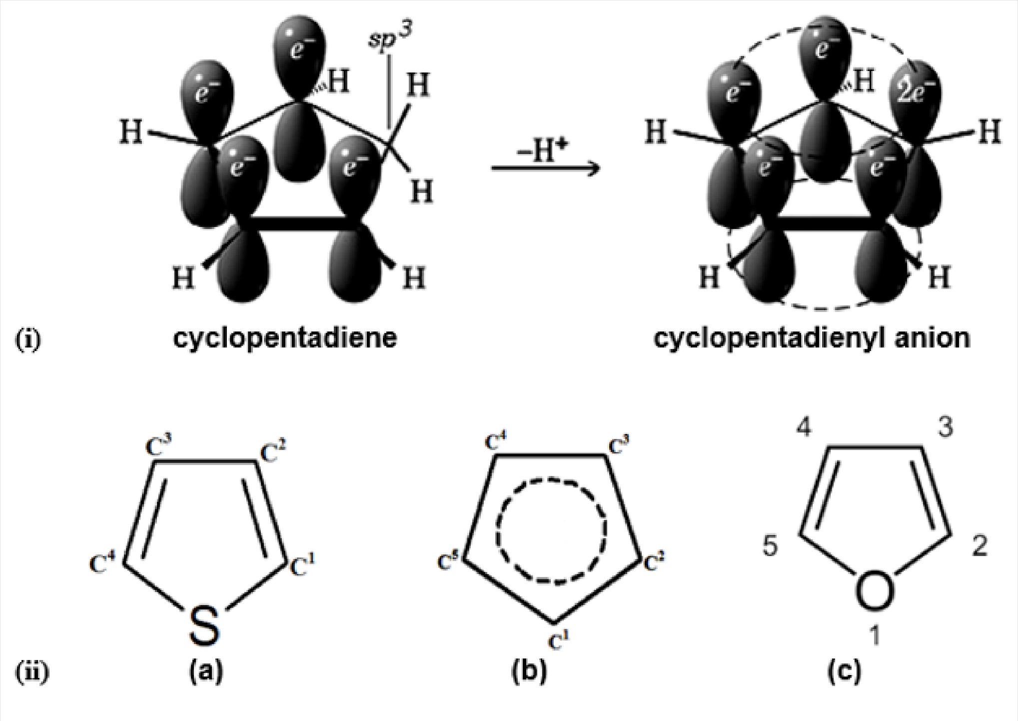

Figure 9: (i) Formation of the resonance in cyclopentadienyl molecule, (ii) atoms used in the superposition.

(a) Thiophene structure (point group C2v),

(b) cyclopentadienyl molecule (point group D5h), its atoms used for superposition are labeled and finally

(c) furan structure (point group C2v).

The sp^2 carbon of the cyclopentadienyl anion (quantified by the similarity indexes with respect to thiophene ring) shows a strong acidic character. These particular facts generate the electronic (dis) similarity of carbon with respect to sulphur in thiophene ring. If all the carbons are sp^2 hybridized, then we have four electrons remaining for pi bonding. Sulphur atom has two lone pairs and two bonds (which would normally make four sp^3 hybridized orbitals). If sulphur one of its lone pairs are promoted to a p orbital it could become hybridized like all the other carbons (three sp^2 and one p) and as a result, there would be (4n + 2) electrons from sulphur atom in the pi bonding. These details generate the (dis)similarity electronic of carbon atom (C) with respect to sulphur (S) in thiophene molecule. In (Figure 10), we can see the contrast of the electronic properties for cyclopentadienyl. These have more anionic characteristic in their behavior, according with the rule of (4n + 2 electrons) in the thiophene. The sp^2 carbon of cyclopentadienyl (quantified by the overlap local index of similarity with respect to the thiophene) is more acidic than we expected (as the alcohol acid character) because the conjugate base, the cyclopentadienyl anion is aromatic and therefore very stable.

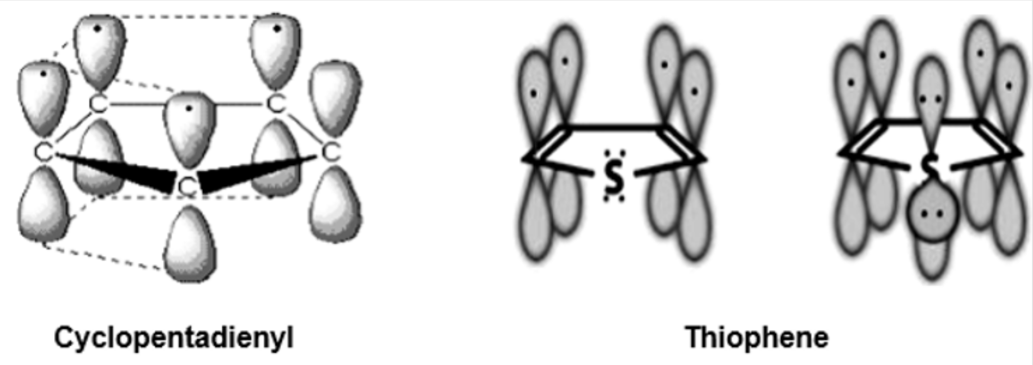

Figure 10: Comparison of the resonant systems of thiophene with respect to the cyclopentadienyl.

The euclidean distances of overlap are higher than the corresponding coulomb distances (Table 4). The bond lengths in the structures (Figure 11) and their respective resonant systems (Figure 1 & 4) have significant differences. This is evidenced by the low value in the local similarity index of overlap with respect to the coulomb index. The trends of the dipole moment and total atomic charges are displayed in (Figure 12). In the case of thiophene the dipole moment is oriented toward the sulphur atom, although it has similar electronegativity to the carbon atom (Pauling electronegativity χ(C): 2.55 and χ(S): 2.58). This small difference causes a decrease of orbital symmetry in the sulphur atom. In this case, it is most probable to find the electron pair near the sulphur atom. The dipole moment in the thiophene is influenced by resonance (Figure 12). The effect of resonance is obviously not sufficient enough to exceed the effect of the electronegativity of sulphur. Thus, the negative pole is located at the heteroatom. However, due to the resonance, the dipole moments of thiophene are smaller than that of the corresponding saturated tetrahydrothiophene. In (Table 5) the higher polarization values are to the thiophene the trend for the dipolar moments of (Figure 12) also were obtain in P-cyclopentadienyl, furan and pyrrole, therefore as a generalization of this is shows the (Figure 13). In (Figure 13 (a)) we can see the polarization relations determined by the equation 41 to thiophene with respect to cyclopentadienyl and the generalization is shows in (Figure 13 (b)), where X is the heteroatom in the heterocycles studied. We expect that in the future this methodology can be applied to a wide range of compounds with major structural differences [96-98] and can also be used towards the better understanding of the inductive effect in polar covalent bonds with external perturbation (Table 6). Additionally, this study is complementary to the studies development by Morales-Bayuelo et al. [95] to understand the distortion of local orbitals by effects of an external electric field using the Hückel method, taking into account the charge transfer on the molecules by polarization effects according to Parr et al. [99].

Table 4: Local Similarity indexes (Numerical and Analytical Method) and euclidean distancies, using global densities for thiophene, furan versus cyclopentadienyl.

Cyclopentadienyl [a]	**$Z_{CP}\,(O)$** [b]	**$Z_{CP}\,(C)$** [c]	**LSI(O)** [d]	**LSI(C)** [e]	**$D_{CP}\,(O)$** [f]	**$D_{CP}\,(C)$** [g]
Thiophene [h]	2.994	196.350	0.972	0.997	0.410	0.966
Vs Furan [h]	3.441	211.863	0.912	0.991	0.871	2.009

[a] Point Group D5h

[b] Interaction of Overlap-Numerical Method

[c] Interaction of Coulomb-Numerical Method

[d] Local Similarity Index of Overlap (see appendix 3)

[e] Local Similarity Índex of Coulomb (see appendix 3)

[f] Euclidean Distance of Overlap

[g] Euclidean Distance of Coulomb

[h] Point Group C2v

Table 5: Induced Molecular Polarity Index proposed for the Thiophene and Furan (PkB) as function of the induce molecular Polarity of cyclopentadienyl (PkA), respectively.

Induced Molecular Polarity Index for Thiophene and Furan P_{kB}:					
2.994 $P_{kA}^{a,b}$	**196.350** $P_{kA}^{a,c}$	**0.972** P_{kA}^{d}	0.997 P_{kA}^{e}	0.410 P_{kA}^{f}	**0.966** $P_{kA}^{d,e}$
3.441 P_{kA}	**211.863** P_{kA}	**0.912** P_{kA}	**0.991** P_{kA}	**0.871** P_{kA}	**2.009** P_{kA}^{f}

Note: k is the quantum states (appendix 1).

[a] Analytical Method

[b] Interaction of Overlap

[c] Interaction of Coulomb

[d] Local Similarity Index of Overlap (see appendix 3)

[e] Local Similarity Index of Coulomb (see appendix 3)

[f] Euclidean Distance of Overlap

[d] Euclidean Distance of Coulomb

[e] Induced Molecular Polarity Index for thiophene

[f] Induced Molecular Polarity Index for furan

PkA: EQ. 7. With respect to the Polarization states (appendix 2)

Table 6: Local Similarity Index (Both Analytical and Numerical Method) and euclidean Distance, using Global Densities for the Pyrrole Vs Cyclopentadienyl.

Structure	**$Z_{CP}(O)^{c}$**	**$Z_{CP}(C)^{d}$**	**$LSI(O)^{e}$**	**$LSI(C)^{f}$**	**$D_{CP}(O)^{g}$**	**$D_{CP}(C)^{h}$**
Pyrrole [a] Vs Cyclopentadienyl [b]	**3.355**	**203.536**	**0.978**	**0.998**	**0.427**	**1.256**

[a] Point Group C2v

[b] Point Group D5h

[c] Interaction of Overlap

[d] Interaction of Coulomb

[e] Local Similarity Index of Overlap

[f] Local Similarity Index of Coulomb

[g] Euclidean Distance of Overlap

[h] Euclidean Distance of Coulomb

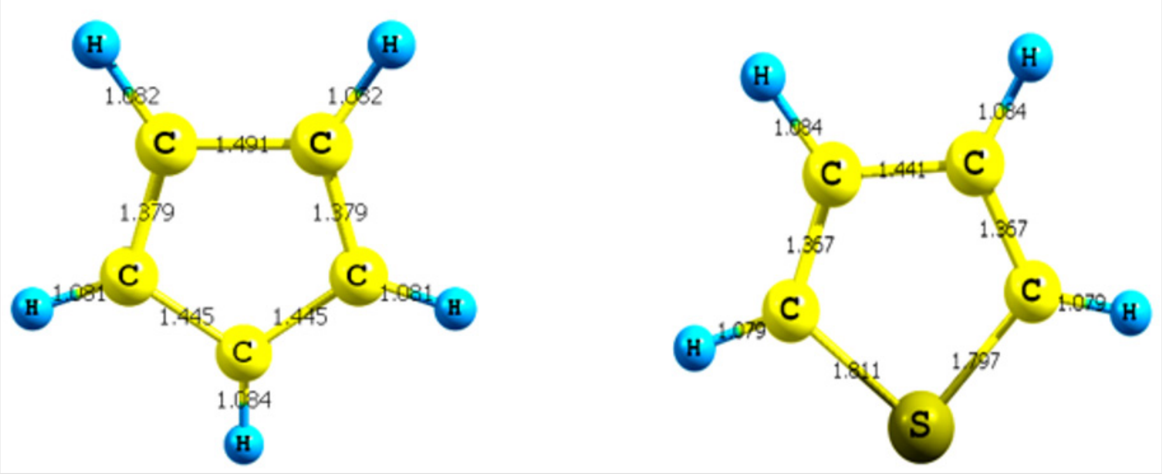

Figure 11: Comparison of the bond distances (Å) of

(a) cyclopentadienyl and

(b) Thiophene.

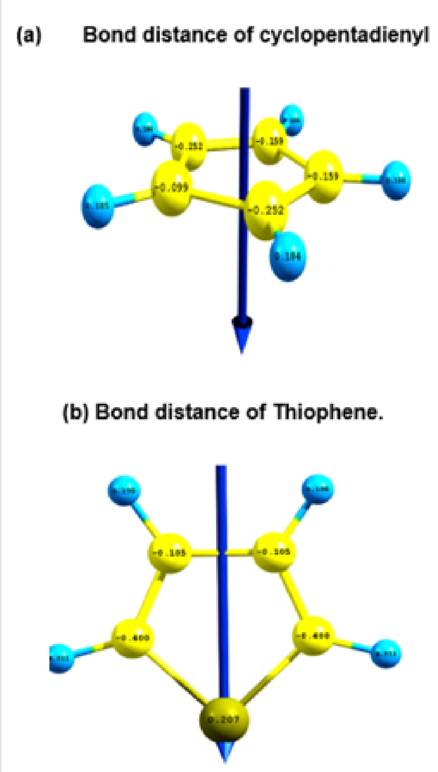

Figure 12: Dipole moment and total atomic charges

(a) cyclopentadienyl molecules and

(b) Thiophene molecule [25].

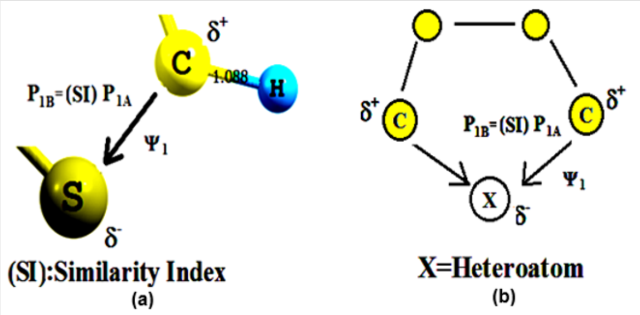

Figure 13:

(a) Molecular polarization descriptor proposed (equation 41) for the state 1 of the (appendix 1), see Table 5.

(b) Generalization of the molecular polarization to the heterocycles studied [25].

Finally, in (Tables 6 & 7) are showed the similarity indexes of pyrrole and pentalene (dimmer system) with respect to cyclopentadienyl (Figure 1). The pyrrole is other heterocyclic aromatic as the furan and thiophene, whereas the pentalene is the dimmer of cyclopentadienyl anion. In (Table 6) we see a local similarity index Overlap of 0.978 and of Coulomb 0.998. It indice allows us to say that the effects associated with the structure as bond distance, atomic size and hybridization sp^2 of the atom nitrogen with respect to the some hybridization of atom carbon in the cyclopentadienyl, are more appreciable that electronic effects as the location of the resonant system, and presence of an additional electron ring Pyrrole with respect to the cyclopentadienyl ring, such results can be checked with their Euclidean distances that for the local similarity index Overlap is 0.427 and for the local similarity index Coulomb is 1.256.

In (Table 6) we can see that the euclidean distance of overlap are higher with respect to the Coulomb distance, this is due to that the bond distances of both structures vary between themselves rather than mutual resonant systems, and this is evidenced by the lower value of index local similarity of overlap with respect to the Coulomb. In (Figure 14), we can see different distances from the carbon-carbon cyclopentadienyl with respect to the distances between the nitrogen-carbon of the pyrrole, which give rise to different molecular polarizations. In (Table 7) we see a local index Overlap of 0.998 and of Coulomb 0.999, this allows us say that the effects associated with the structure, such as bond distance are quantify in good form with the TGSA program to the cyclopentadienyl with respect pentalene dimmer of Cyclopentadiene. Therefore, it dimmer not alter the overlapping atomic structural with respect to the cyclopentadienyl, (Figure 15).

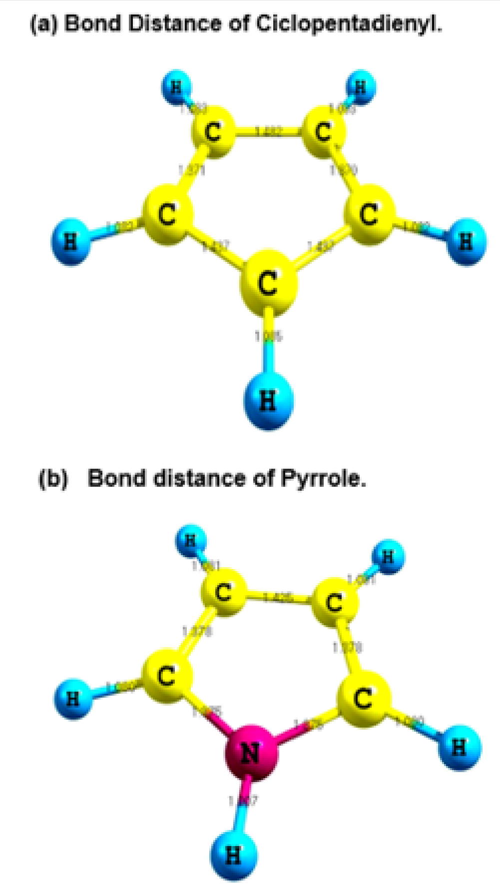

Figure 14: Comparison of bond distances in Armstrong units (Å) of

(a) Ciclopentadienyl and

(b) Pyrrole.

DOI: 10.26717/BJSTR.2020.25.004187

Table 7: Local Similarity Index (Both Analytical and Numerical Method) and euclidean Distance, using global densities for the pentalene Vs cyclopentadienyl

Structure	Z_{CP} (O)[c]	Z_{CP} (C)[d]	LSI(O)[e]	LSI(C)[f]	D_{CP} (O)[g]	D_{CP} (C)[h]
Pentalene [a] Vs cyclopentadienyl[b]	29.439	616.125	0.998	0.999	2.257	10.662

[a] Point Group C2h

[b] Point Group D5h

[c] Interaction of Overlap

[d] Interaction of Coulomb

[e] Local Similarity Index of Overlap

[f] Local Similarity Index of Coulomb

[g] Euclidean Distance of Overlap

[h] Euclidean Distance of Coulomb

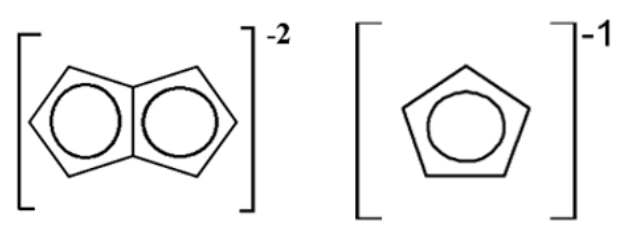

Figure 15: Comparison of the resonant systems of pentalene with respect to the cyclopentadienyl [25].

(Figure 15) shows as the pentalene can be considered as the dimmer formed by two cyclopentadienyl rings (dianion) [100,101], so the resonance in the cyclopentadienyl anions are presented also in its dimeric form (Figure 4). In (Figure 16) is shows the different distances from the carbon-carbon bond in the cyclopentadienyl and the distances between the carbons in the pentalene, which give rise to different molecular polarizations, also in this figure shows that the distances between the atoms of the bonds on the actual structure of cyclopentadienyl compared with those of pentalene are slightly similar. Finally, in (Tables 8 & 9) is shows the energies of the orbitals of pyrrole and pentalene as a function of the energies of cyclopentadienyl, obtaining degenerate values, considering their local indexes of similarity.

Table 8: Values of energy orbital of Pyrrole as a function of orbital energies of cyclopentadienyl, for each descriptor of Similarity.

Energy values	LSI(O)[a]	LSI(C)[b]	D_{CP} (O)[c]	D_{CP} (C)[d]
E_1	$0.978\alpha + 1.956\beta$	$0.998\alpha + 1.996\beta$	$0.427\alpha - 0.854\beta$	$1.256\alpha + 2.512\beta$
E_2	$0.978\alpha - 1.582\beta$	$0.998\alpha + 1.615\beta$	$0.427\alpha - 0.688\beta$	$1.256\alpha - 2.032\beta$
E_3	$0.978\alpha + 0.604\beta$	$0.998\alpha - 0.617\beta$	$0.427\alpha - 0.261\beta$	$1.256\alpha + 0.776\beta$

[a] Local Similarity Index of Overlap

[b] Local Similarity Index of Coulomb

[c] Euclidean Distance of Overlap

[d] Euclidean Distance of Coulomb

Table 9: Values of energy orbital of Pentalene as a function of orbital energies of cyclopentadienyl, for each descriptor of Similarity.

Energy values	LSI(O)[a]	LSI(C)[b]	D_{CP} (O)[c]	D_{CP} (C)[d]
E_1	$0.998\alpha + 1.996\beta$	$0.999\alpha + 1.998\beta$	$2.257\alpha + 4.514\beta$	$10.662\alpha + 21.324\beta$
E_2	$0.998\alpha + 0.617\beta$	$0.999\alpha + 0.617\beta$	$2.257\alpha + 1.395\beta$	$10.662\alpha + 6.589\beta$
E_3	$0.998\alpha + 0.617\beta$	$0.999\alpha + 0.617\beta$	$2.257\alpha + 1.395\beta$	$10.662\alpha + 6.589\beta$
E_4	$0.998\alpha - 1.615\beta$	$0.999\alpha - 1.614\beta$	$2.257\alpha - 3.652\beta$	$10.662\alpha - 17.251\beta$
E_5	$0.998\alpha - 1.615\beta$	$0.999\alpha - 1.614\beta$	$2.257\alpha - 3.652\beta$	$10.662\alpha - 17.251\beta$

DOI: 10.26717/BJSTR.2020.25.004187

[a]Local Similarity Index of Overlap
[b]Local Similarity Index of Coulomb
[c]Euclidean Distance of Overlap
[d]Euclidean Distance of Coulomb

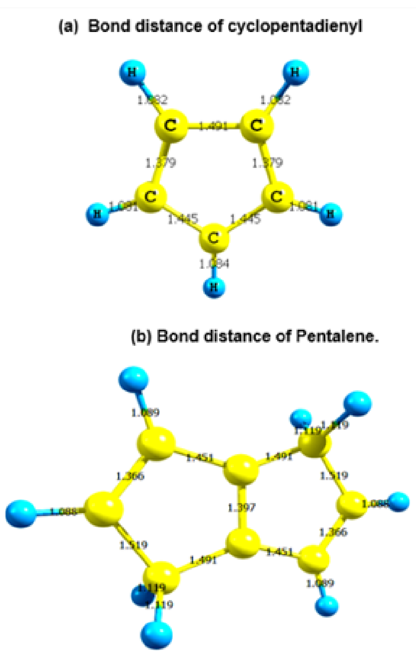

Figure 16: Comparison of the bond distances (Å) of
(a) cyclopentadienyl and
(b) Pentalene [25].

The elevated values of (MQS) indexes (Table 9) are due to the high overlap (Figure 17) that occurs between the pentalene and cyclopentadienyl, taking in account that the pentalene can be seen as its dimeric form, so the electronic and structural features are preserved, allowing to relate their orbital energy. (Figure 17) clearly shows a dependence of the overlap MQSM on the mutual position of both molecules in space. Molecular alignment has important influence on the MQSM. One of the applications of (MQS) is the possibility to quantitatively express the similarity and specially to compare and order the degree of similarity over pairs of molecules, (Figure 17).

Analyzing only at the carbon atoms in the molecules (A and B), the first maximum occurs when the first two atoms a and g in (Figure 17) coincide, the importance of this new techniques lies in the finding of similar characteristics that allow us correlate members, in that sense the ubiquitous nature of the similarity concept is used in this review [102]. Traditionally, the Hückel method has good applications in reactions governed by the WH rules as the DA reactions, for this reason a study to analyze the stability of the new insights on the Hückel method reported in this review is developement using a heterocyclic of (Figure 1) as furan. In this regard, a series of cycloaddition reactions between masked *o*-Benzoquinones and furan derivatives (Scheme 1) are studied. Additionally, these reactions involve dipole-dipolarophiles interactions, which have important effects on the molecular polarization and can yield information on the molecular topological space.

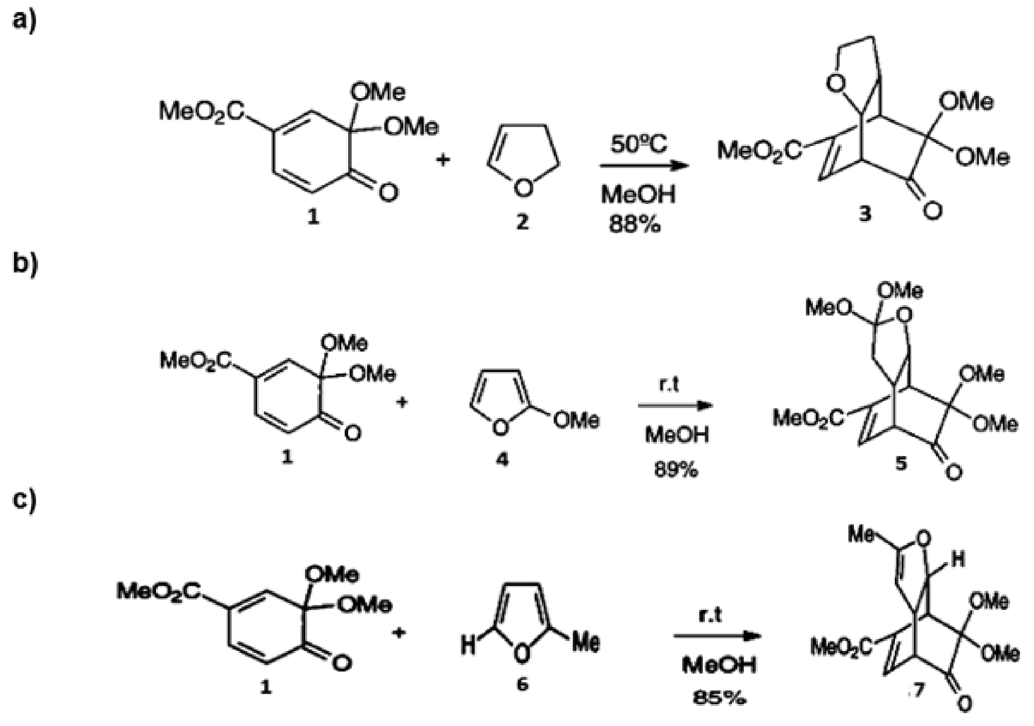

Scheme 1: Diels-Alder Cycloadditions [2], furan derivatives (Compounds 2, 4 and 6) and Masked o-Benzoquinone (compound MOB 1) are used to propose topological descriptors of reactivity using (DFT) and (MQS).

DOI: 10.26717/BJSTR.2020.25.004187

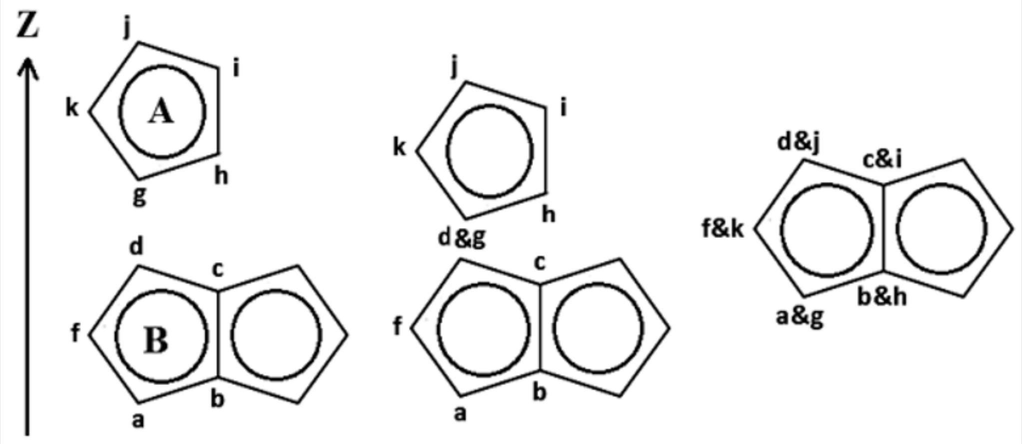

Figure 17: The molecules cyclopentadienyl (A) and Pentalene (B). A is moved along the Z-axis producing higher spatial overlap with B.

Hückel method in the topological analysis using Molecular Quantum Similarity (MQS) and chemical reactivity descriptors.

In this issue, the extended Hückel method is related with the topological analysis and is one important tool in the molecular topology moreover the graph-theoretical approach is often a restatement of Hückel molecular orbital theory. For this reason, in this Computational Review a topological study is postulate using the Hückel method proposed on the DA reactions. Is very well know that the Carbó and Hodgkin-Richards index dependent on the relative orientation of the molecules studied, taking into account that due to this dependence has been proposed many methods of alignment, ranging from methods such as Comparative Molecular Similarity Indexes Analysis (CoMSIA) and Comparative Molecular Field Analysis (CoMFA) which are in three dimensions and allows obtain maps steric, electrostatic, hydrophobic among others [103], these methods have been proposed in order to find alignment patterns that yield the best results by aligning structures, to find the most optimal method that allows obtain the best values of the similarity indexes.

In the present dissertation also was used the (**TGSA**) alignment method [104], this algorithm is based on comparison of the types of atoms and distances between them. TGSA can be used for systems with some common (sub)structure and can align similar functional groups between molecules under comparison in a way consistent with the experimental results. In this work on the topological method was studied a molecular set with the particularity that it has a structural fragment common to all structures and this common fragment is also a molecule and not a portion or structural fragment of one of them (Figure 18).

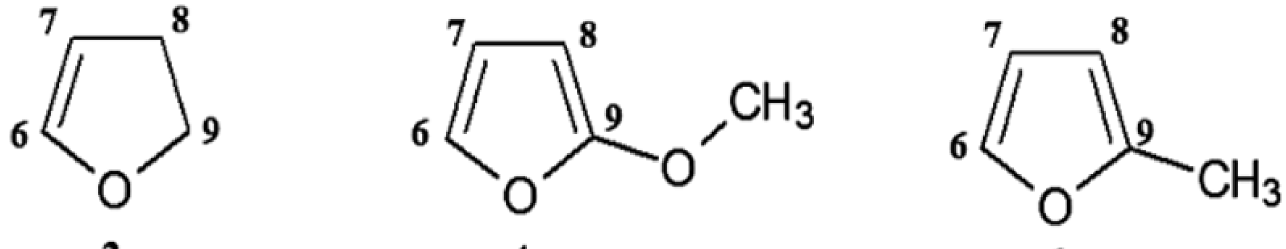

2

4

6

Figure 18: Structure of the Compound dihydrofuran 2, Compound 4 and 6, the compound 2 is used for the alignment with the Topo-Geometrical Superposition Approach (TGSA).

The topological analysis of electron density was performed by Bader in the 90's, who analyzed the field gradient of the density of electrons in order to conceptualize an atom in a molecule [105]. The conditions of the (FF) was postulated by Chattaraj et al. [106], which proposes an expansion of the gradient of the function of Fukui, recently calculated by Ayers and Levy [106]. The interatomic distances among the atoms of the compounds 2, 4 and 6 are analyzed in (Figure 19). The C-C bond distances of these molecular set are different in these molecules. So, we can assume that this difference or (dis)similarity is due to the presence of substituent groups on compounds 4 and 6 with respect to compound 2. For this reason, in this contribution is proposed a topological analysis characterized by the calculation of Molecular Quantum Similarity Local Atomic (MQSLA) through the multiplication of MQS index of Carbó with MQSLA using equations (10)–(15) by the absolute value of the total atomic charges shown in the (Figure 20), using equation 48 to the calculate of the local atomic similarities of the compounds 4 and 6 with respect to compound 2. These results are depicted in (Tables 10), using the values of the (MQS) of the (Table 11).

Table 10: Similarity Index (Both Analytical and Numerical Method) and euclidean Distance, using Global Densities for the 2 versus 4 and 6.

Molecule (2)[a]	**Z(*O*)[b]**	**Z(*C*)[c]**	**SI(*O*)[d]**	**SI(*C*)[e]**	**D_{CP} (*O*)[f]**	**D_{CP} (*C*)[g]**
4	4.439	265.142	0.783	0.897	1.648	7.488
6	5.449	339.606	0.897	0.979	1.007	3.749

[a] Scheme 1

[b] Interaction of Overlap

[c] Interaction of Coulomb

[d] Similarity Index of Overlap

[e] Similarity Index of Coulomb

[f] Euclidean Distance of Overlap

[g] Euclidean Distance of Coulomb

Table 11: Calculation of (MQSM) local atomic (MQSLA) EQ [48].

Compound 2[a] vs Compound 4	**Z(*O*)[b]**	**Z(*C*)[c]**	**SI(*O*)[d]**	**SI(*C*)[e]**	**D_{CP} (*O*)[f]**	**D_{CP} (*C*)[g]**
$R^{local}_{c^2c^9}$	**0.169**	**10.075**	**0.029**	**0.034**	**0.063**	**0.285**
$R^{local}_{c^2c^8}$	**0.657**	**39.241**	**0.116**	**0.133**	**0.244**	**1.108**
$R^{local}_{c^2c^7}$	**1.252**	**74.770**	**0.221**	**0.252**	**0.465**	**2.111**
$R^{local}_{c^2c^6}$	**0.080**	**4.772**	**0.014**	**0.016**	**0.029**	**0.134**
Compound 2[a] vs Compound 6						
$R^{local}_{c^2c^9}$	**0.207**	**12.905**	**0.034**	**0.037**	**0.038**	**0.142**
$R^{local}_{c^2c^8}$	**0.806**	**50.262**	**0.133**	**0.145**	**0.149**	**0.555**
$R^{local}_{c^2c^7}$	**1.537**	**95.769**	**0.253**	**0.276**	**0.284**	**1.057**
$R^{local}_{c^2c^6}$	**0.098**	**6.112**	**0.016**	**0.018**	**0.018**	**0.067**

[a] Scheme 1

[b] Interaction of Overlap

[c] Interaction of Coulomb

[d] Similarity Index of Overlap

[e] Similarity Index of Coulomb

[f] Euclidean Distance of Overlap

[g] Euclidean Distance of Coulomb

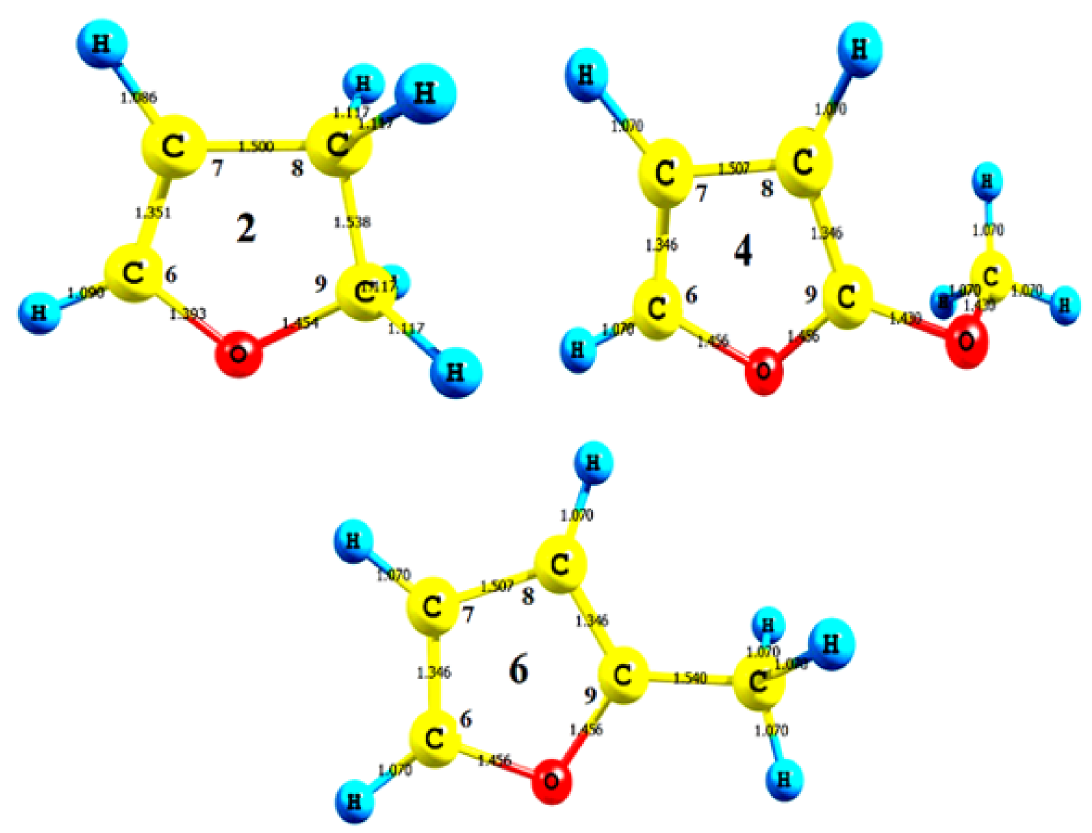

Figure 19: Bond Lengths (Å), for the Compounds 2, 4 and 6, using Chemcraft 1.6 program.

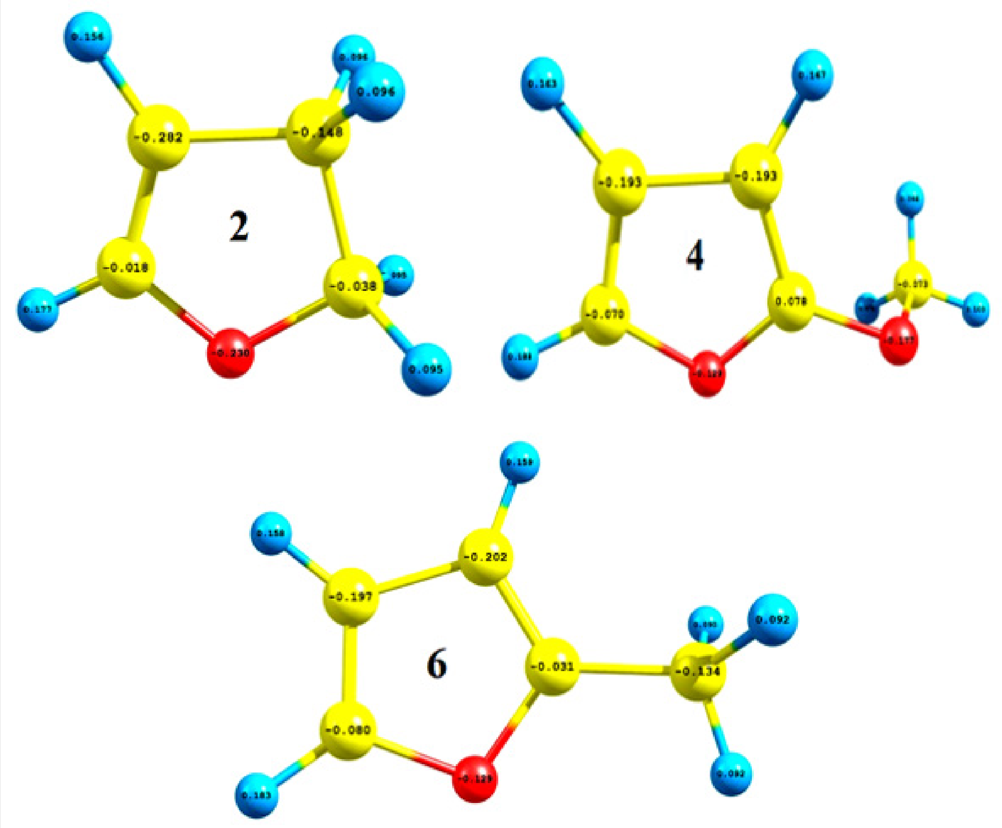

Figure 20: Total atomic charges, for the Compounds 2, 4 and 6 [25].

$$R^{local-Atomic}_{c^2c^n} = \mathrm{MQSLA}\left|C.\,Atomic\right| \qquad (48)$$

where n = 6,7,8,9, represent the positions of the local carbon atoms analyzed according to the numbering used for the molecular alignment using TGSA approach (Figure 18). Considering that the compounds analyzed 4 and 6 are derivatives of dihydrofuran 2. We used the equation 48 in order to calculate the local atomic physicochemical descriptor which can describe the atomic charges of the compounds 4 and 6 with respect to compound 2, so that equation 48 allows us to quantify the MQSLA. The molecular structure of compound 2 (Table 11) has more similarity with the molecule 6 quantified by quantum similarity index of overlap 0.897 and the Coulomb 0.979, comparing these two values shows that the Coulomb index is the best descriptor of similarity in comparison with the of Overlap value, taking into account that naturally the Carbó index is limited to the range (0, 1), where C_{AB} = 1 means Self-Similarity. On the other hand, the structures considered in this study are derived from dihydrofuran 2.

Additionally, to the calculation of MQSLA values, in this Computational Review we propose a topological analysis based on the multiplication of global reactivity indexes (electrophilic chemical potential and chemical hardness) with MQS indexes, using the following equations:

$$\omega_{2k} \approx \omega R^{local}_{c^2c^n} \approx \frac{\mu^2}{2\eta} R^{local-Atomic}_{c^2c^n} \qquad (49)$$

$$\mu_{2k} \approx \mu R^{local}_{c^2c^n} \approx (\varepsilon_H + \varepsilon_L) R^{local-Atomic}_{c^2c^n} \qquad (50)$$

$$\eta_{2k} \approx \eta R^{local}_{c^2c^n} \approx (\varepsilon_L - \varepsilon_H) R^{local-Atomic}_{c^2c^n} \qquad (51)$$

Where n= 9,8,7,6 and 2k=(Compound 2)(Compounds 4 and 6), these equations (**49-52**) represent the similarity in molecules fragments, taking into account the differences of 4 and 6 with 2 is that are derived from furan, so all contributions of similarity in structures 4 and 6, can be quantified on a local the carbon atom C2 (Scheme 1), and from that point of view allows us to express the reactivity indexes of global and local contributions, and performing topological considerations of the electron density. In this method, we propose that the chemical potential, hardness and electrophilicity total formed by the sum of carbon atoms of the compounds analyzed 4 and 6 with respect to compound 2, is given by equation 52.

$$U_{2kJ} : \sum_{n:6}^{9} R^{local-Atomic}_{c^2c^n} \qquad (52)$$

Where *U*: μ, η, ω, 2k: (Compound 2) (Compounds 4 and 6), and *J*: (O: Overlap and C: Coulomb, respectively); these results are shown in (Table 11), the total reactivity descriptor provides considerations about the reactivity of the system-C8 C6-C7 -C9, used for the analysis proposed in this review.

Topological Similarity analysis proposed: global reactivity indexes as local in Diels-Alder Reactions

In the reference [107] is presented an analysis of the Potential Energy Surfaces (PES) for the reaction between masked o-benzoquinone (MOB) and compound 6, indicating that this reaction takes place along of a mechanism stepwise (Figure 21), this mechanism is initiated by the nucleophilic attack of the carbon atom unsubstituted C6 of 2-methylfuran to the C5 carbon atom of an intermediary Zwitterion MOB1, occasionally happen after the Cyclization of the intermediate along the formation of a new C-C bond, to obtain the final product (Channel TS1-en). In (Table 13), is shown the electronic chemical potential MOB1 (μ=-0.1674 au, for the Compound 1) is less than the chemical potential of compound 6 (μ=-0.0946 au). Taking into account that the two stereoisomeric reactive channels (the attack on the ortho and meta position) are possible for the furan derivatives (Figure 21), the C6 position of 2-methylfuran is more nucleophilic [107] discarding the study in the C7 position of the compound 2 in the conjugated position MOB2 C5 [107]. With this experimental and theoretical evidence, we calculated the MQS indexes local (Table 11), using LMQSI: Overlap-Interaction, Coulomb-Interaction, similarity Overlap, Coulomb similarity, and euclidean distances of Overlap and Coulomb, respectively.

Table 12: Shows the states global properties, for derivativos of furan studied (2, 4 and 6).

Molecule	μ	η	ω
1	-0.167	0.145	2.62
2	-0.080	0.247	0.36
4	-0.079	0.229	0.37
6	-0.094	0.236	0.52

[a] Electronic chemical potential, (au), and chemical hardness, values are in atomic units; electrophilicity power values, are in electronvolts. Ref. [101].

Table 13: Static local properties proposed, for derivatives of furan studied (2, 4 and 6), using Eqs [49-51].

3	Z(*O*)[b]	Z(*C*)[c]	SI(*O*)[d]	SI(*C*)[e]	$\lvert D_{CP}$ (O)$\rvert$[f]	$\lvert D_{CP}$ (C)$\rvert$[g]
$\mu_{24}R^{local}_{c^2c^9}$	-0.013	-0.809	-0.230*	-0.270*	0.500*	0.023
$\mu_{24}R^{local}_{c^2c^8}$	-0.052	-3.151	-0.930*	-0.011	0.020	0.089
$\mu_{24}R^{local}_{c^2c^7}$	-0.101	-6.004	-0.017	-0.020	0.037	0.169
$\mu_{24}R^{local}_{c^2c^6}$	-0.640*	-0.383	-0.110*	-0.120*	0.230*	0.011
Compound 2[a] vs Compound 6						
$\mu_{26}R^{local}_{c^2c^9}$	-0.017	-1.032	-0.270*	-0.300*	0.300*	0.011
$\mu_{26}R^{local}_{c^2c^8}$	-0.064	-4.021	-0.010	-0.012	0.012	0.044
$\mu_{26}R^{local}_{c^2c^7}$	-0.122	-7.662	-0.020	-0.022	0.023	0.085
$\mu_{26}R^{local}_{c^2c^6}$	-0.780*	-0.489	-0.130*	-0.140*	0.140*	0.540*
Compound 2[a] vs Compound 4						
$\eta_{24}R^{local}_{c^2c^9}$	0.042	2.489	0.730*	0.840*	0.016	0.070
$\eta_{24}R^{local}_{c^2c^8}$	0.162	9.693	0.029	0.032	0.060	0.274
$\eta_{24}R^{local}_{c^2c^7}$	0.309	18.468	0.055	0.062	0.114	0.521
$\eta_{24}R^{local}_{c^2c^6}$	0.019	1.786	0.350*	0.400*	0.720*	0.033
Compound 2[a] vs Compound 6						
$\eta_{26}R^{local}_{c^2c^9}$	0.051	3.187	0.840*	0.910*	0.930*	0.035
$\eta_{26}R^{local}_{c^2c^8}$	0.199	12.415	0.033	0.036	0.037	0.137
$\eta_{26}R^{local}_{c^2c^7}$	0.380	23.655	0.062	0.068	0.070	0.261
$\eta_{26}R^{local}_{c^2c^6}$	0.024	1.509	0.400*	0.440*	0.440*	0.017
Compound 2[a] vs Compound 4						

$\omega_{24}R^{local}_{c^2c^9}$	**0.060**	**3.627**	**0.010**	**0.012**	**0.023**	**0.103**
$\omega_{24}R^{local}_{c^2c^8}$	**0.237**	**14.127**	**0.402**	**0.048**	**0.089**	**0.399**
$\omega_{24}R^{local}_{c^2c^7}$	**0.451**	**26.92**	**0.080**	**0.090**	**0.167**	**0.756**
$\omega_{24}R^{local}_{c^2c^6}$	**0.028**	**1.718**	**0.500***	**0.580***	**0.010**	**0.048**
Compound 2[a] vs Compound 6						
$\omega_{26}R^{local}_{c^2c^9}$	**0.048**	**4.646**	**0.034**	**0.013**	**0.013**	**0.051**
$\omega_{26}R^{local}_{c^2c^8}$	**0.290**	**18.094**	**0.048**	**0.052**	**0.149**	**0.199**
$\omega_{26}R^{local}_{c^2c^7}$	**0.553**	**34.477**	**0.091**	**0.099**	**0.102**	**0.381**
$\omega_{26}R^{local}_{c^2c^6}$	**0.035**	**2.200**	**0.500***	**0.650***	**0.650***	**0.024**

Noté: The Electronic chemical potential () is taken as Absolute valué, expressing the global reactivity Index With respect to the Euclidians Distance between the reactants.

[a]Scheme 1

*(Multiplied by 102)

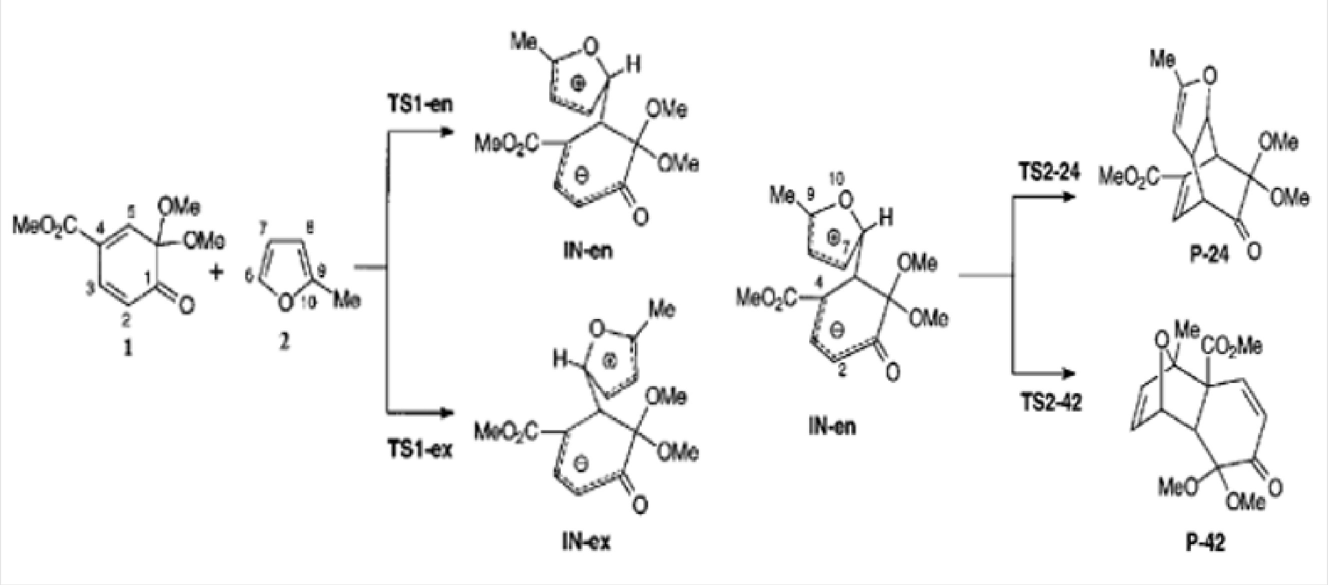

Figure 21: Two of the possible stereochemical pathways of reactivity between the Compound 1 and 2:

(i) The initial attack of compound 2 to 1, corresponding to the endo and exo approach of 2-methylfuran to the position 3 belonging to the diene system MOB1, the product P-24: cycloaddition {2+4} and

(ii) (ii) Via P-42 is the cycloaddition {4 +2}. Reference [101].

Two of the possible stereochemical pathways of reactivity between the Compound 1 and 2:

(i) The initial attack of compound 2 to 1, corresponding to the endo and exo approach of 2-methylfuran to the position 3 belonging to the diene system MOB1, the product P-24: cycloaddition {2+4} and

(ii) **(ii)** Via P-42 is the cycloaddition {4 +2}. Reference [107] In (Figure 22) are depicted the local reactivity indexes of Fukui, which represent susceptibility electrophilic species attack, ref. [107], for the cycloaddition studied (Scheme 1). The (Table 14) shows the values of chemical potential proposed for compounds 4 and 6, note that in all cases the values of $\mu_{2n}R^{local}_{c^2c^6}$ are garetear than $\mu_{2n}R^{local}_{c^2c^9}$, whereas n: componed 4 and 6, are in agreement with the stereochemical preference as is depicted in (Figure 21), which means that the carbon atom (C6) is more similar than the carbon atom (C9) to allow electrons to flow from the electron cloud, which agrees with observed values of Fukui (FF$^-$), this is manifesting in increased susceptibility to form bonds with the MOB 1, the same trend is observed in hardness and electrophilicity index proposed, therefore we can say that the C6 position consistently has the lowest energy of stabilization when it is capable of receiving electrons from the MOB 1.

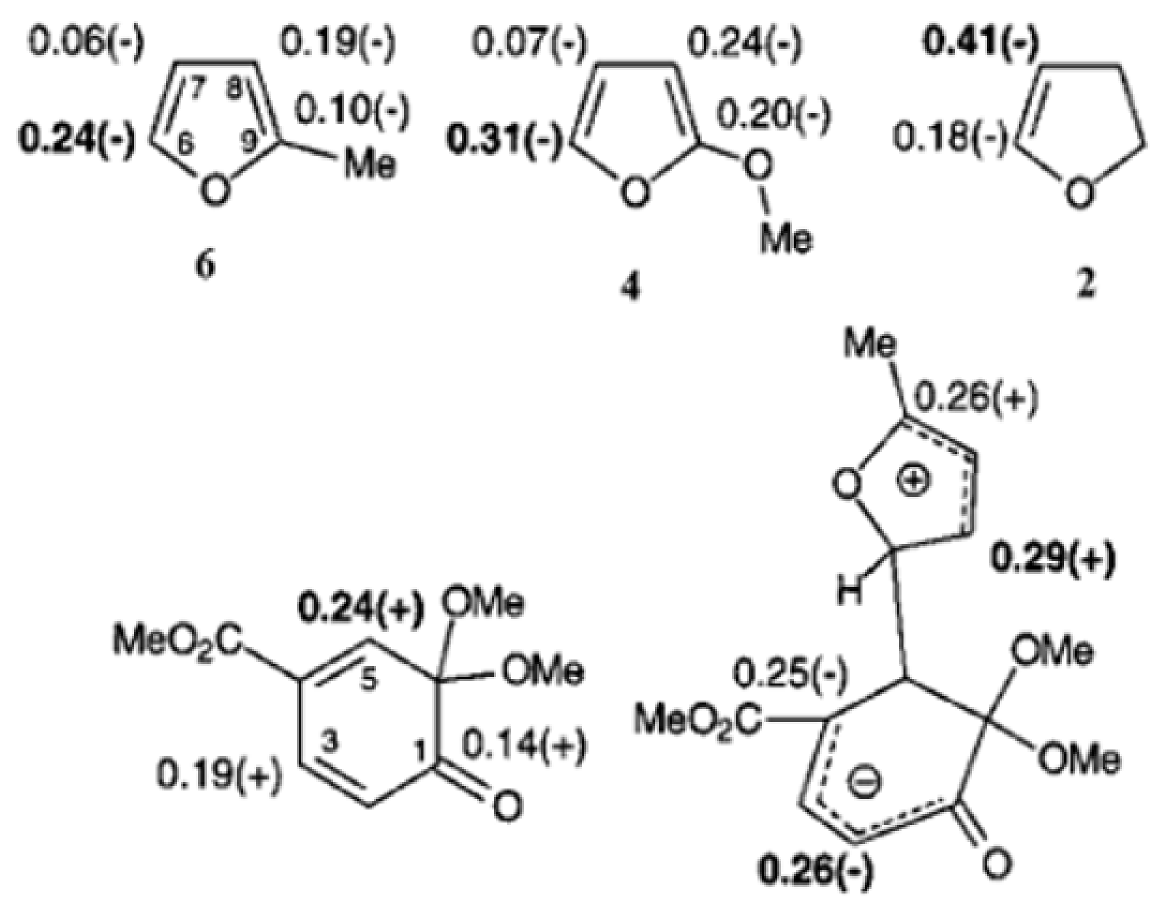

Figure 22: Fukui functions for electrophilic (-) attacks for the furan derivatives 2, 4, and 6, and the intermediate IN-en of Channel TS1-en (Figure 21), the values higher in the Fukui functions are shown in bold [101].

Table 14: Proposed total reactivity descriptors, calculated With the equation [49-52].

Molecule	$Overlap(\mu_{TO})$	$Coulomb(\mu_{TC})$	$Overlap(\eta_{TO})$	$Coulomb(\eta_{TC})$	$Overlap(\omega_{TO})$	$Coulomb(\omega_{TC})$
22	-0.039	-0.039	0.247	0.247	0.360	0.360
24	-0.030	-0.035	0.590	0.106	0.497	0.156
26	-0.034	-0.038	0.107	0.118	0.178	0.270

Comparing the hardness values (Table 14) of the carbon atom C6 and C9 of the compounds 4 and 6, show that the hardness values on the C9 is greater than the C6 atom indicating that the C6 carbon atom has the higher opposition to distort the electron cloud formation favoring the formation of a bond with MOB1, which allows us to say that these dihydrofuran derivatives have similar chemical behavior, which are confirmed by the Fukui functions (Figure 22), this is a reason more for the inclusion of the quantum similarity in the chemical reactivity field, taking into account that the search for methods to explain the pericyclic reactions is an area of continuing interest [101-103].

Analyzing compound 2, we can see different results with respect to compounds 4 and 6. For instant the greatest value of the (FF) in the compound 2 is at the C7 carbon atom meanwhile to compounds 4 and 6 is on carbon 6 (Figure 22). This result is in agreement with data shown in (Table 15), because the local electrophilic self-similarity proposed for these derivatives can be associated with carbon atoms C6 and C7 with a value of ($\omega_k = 0.36eV$) for reactivity descriptors proposed of overlap and coulomb, the maximum value ω_{TO} is observed when compared the compound 2 with 4 and the lower value is when compared 2 with 6, which agrees with the structural characteristics, different case is observed in the value of ω_{TC} which has the lower value when is compared the compound 4 with 2, the which agrees with the similarity measured by the electronic quantum Coulomb index of compound 2 with 4 (0.897), (Table 14).

The results found in this study are agree with the results reported by Domingo et al. [108] in the analysis of the (FF) and also in agreement with the explanations of unusual meta regioselectivity found in these dihydrofuran derivatives as is showing in (Figure 22), with the ortho regioselectivity of this type of cycloadditions, therefore this complementarity between the Fukui functions and local reactivity indexes that is propose in the present Computational Review (Tables 11 & 14) is consistent with the experimental results. These results lead us to postulate this Computational Review as tool for topological analysis, considering the regioselectivity and stereochemistry associated with this type of cycloaddition.

The total chemical potential proposed and calculated with equation 50 is showed in (Table 15). With values of: $Overlap(\mu_{TO22})$:-0.039, $Overlap(\mu_{TO24})$:-0.030, $Overlap(\mu_{TO26})$:-0.034, and $Coulomb(\mu_{TO22})$:-0.039, $Coulomb(\mu_{TO24})$:-0.035, $Coulomb(\mu_{TO26})$:-0.038, this has the same trends **{4> 6> 2}** that the values found for the Fukui functions for the atom C6 compounds 2, 4 and 6 with values of $f^- : f_2^- : 0.18, f_4^- : 0.31, f_6^- : 0.24$ (Figure 22), considering that the C6 carbon atom is responsible for the preferred stereochemistry, which allow us say that this set of indexes can be considered as local reactivity indexes associated with the carbon atom C6 in addition, this indexes proposed we can associate with the sensibility in the chemical potential of the Fukui functions with respect to the external distributions and can be expressed mathematically by the relationship [53].

$$f(r) = \left[\frac{\delta\mu}{\delta\upsilon(r)}\right]_N \qquad (53)$$

This equation 53 provides the mathematical evidence of the complementarity of the chemical potential with the Fukui functions that was evidenced in the proposed local reactivity indexes. So, we can propose a topological analysis of global indexes as local, this proposal may be an alternative to the condensed version of global reactivity indexes and has the advantage of being mathematically well-defined, avoiding ambiguities in the condensed form of global indexes of reactivity. Comparing (Tables 13 & 14) we can call the global reactivity indexes as relative reactivity indexes, because these are proposed based on (MQS) indexes of the structure 2 with respect at 4 and 6, taking into account that the molecules studied are derivatives of dihydrofuran and relate to each other in a relative way, allowing relate the reactions where these structures are involved (Scheme 1). Due to that the reactions depicted in (Figure 23) have a large ionic character [104] in this study is analyzed the corresponding reagents with their intermediaries, as a consequence the local Fukui functions of the reagents 2, 4, 6, and it is related with the stereochemistry reported for this type of DA cycloaddition through the reactivity indexes proposed.

The (Figure 23) clearly shows a dependence of the MQSM of overlap on the mutual position of both molecules in space. Molecular alignment thus has important influence on the MQSM. One of the applications of MQS is the possibility to quantitatively express the similarity and specially to compare and order the degree of similarity over pairs of molecules, different important characteristics of MQSM may be discerned from (Figure 24). Analyzing only at the carbon atoms in the molecules (A and B), the first maximum occurs when the first two atoms c and f in (Figure 24) coincide, all these orientations give rise to interactions of overlap and coulomb which are quantified by MQS indexes of overlap and coulomb, (Table 11), giving rise to reactivity indexes proposed in this study from the point of view of the interactions produced by the orientations that favor the highest value in the means of similarity taking into account the importance of this new techniques lies in the finding of similar characteristics that allow us to correlate members in organic Physicochemical and study steric and electronic effects in reactions where the extended Hückel method proposed in this review can be applied.

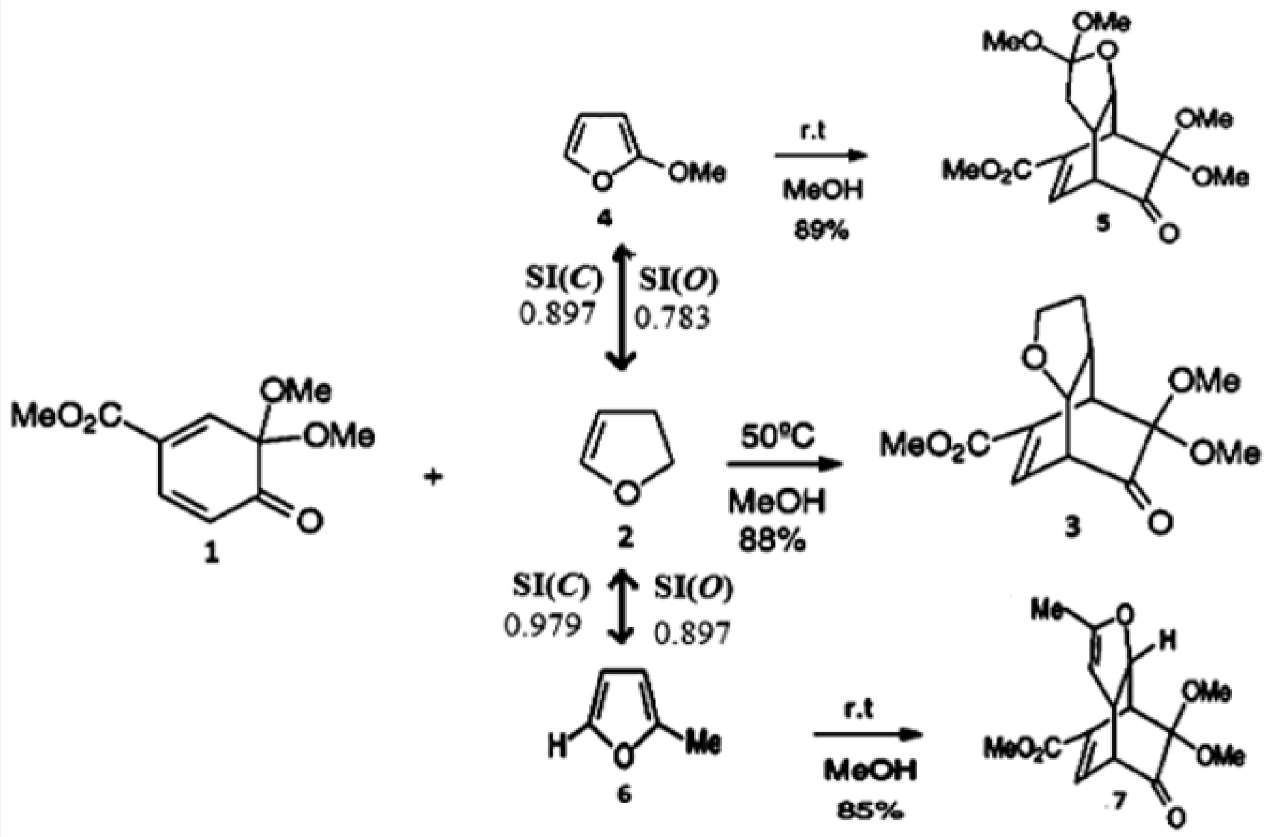

Figure 23: Similarity relations that can express reactivity indexes global as local indexes (Table 13, 14 and 15).

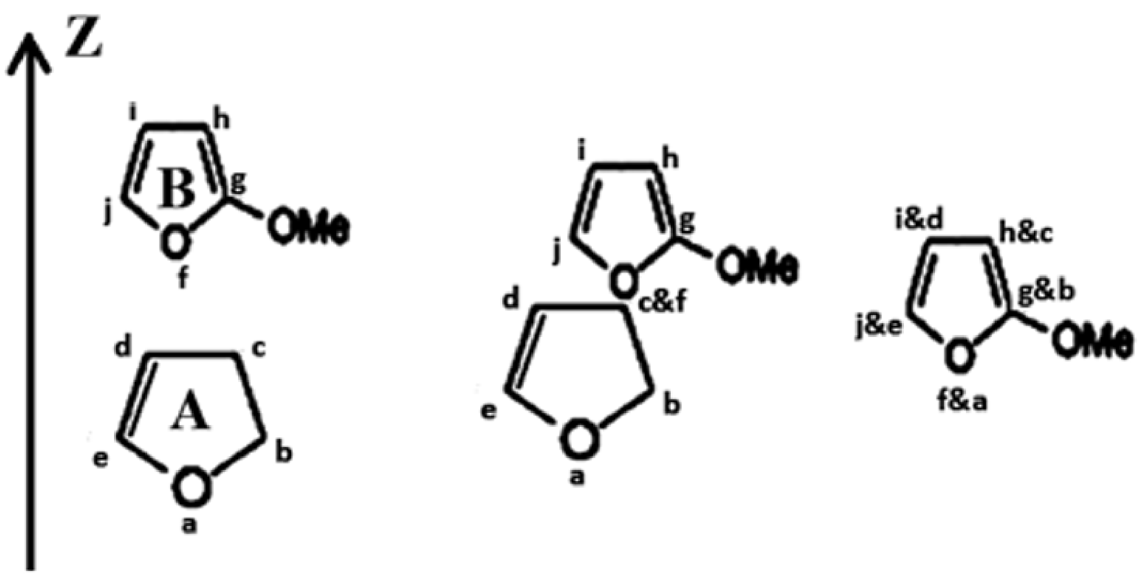

Figure 24: The Compound 2 (A) and Compound 4 (B). A is moved along the Z-axis producing higher spatial overlap with B.

In this sense, this Computational Review provides a convenient way of describing and predicting the molecular structure within the constraints of three-dimensional (3D) space. Given the determinants of chemical bonding and the chemical properties of the atoms, topology provides a model for explaining how the atoms ethereal wave functions must fit together. On the other hand, each scalar field has its own distinctive topology, and each provides different information about the nature of chemical bonding and structure. The analysis of these topologies, when combined with simple electrostatic theory and a few empirical observations, leads to a quantitative model of localized chemical bonding. Therefore, in this methodology, the analysis provides insights into the nature of chemical bonding in π-conjugate systems.

Conclusion

In this Computational Review entitled: extended Hückel method using molecular polarization, quantum similarity and chemical reactivity descriptors supported in the density functional theory, we highlight the following aspects:

Extended Hückel Method Using Molecular Polarization and Molecular Quantum Similarity Aromaticity studies

In this issue, the molecular polarizabilities of heterocyclic systems were presented as a function of polarizability, taken as reference the cyclopentadienyl molecule. Additionally, a new technique to express the energy values of pyrrole, P-cyclopentadiene, thiophene, furan and pentalene as a function of the cyclopentadienyl energies by the introduction of overlap and coulomb local similarity indexes in the secular determinant of the Hückel method, is proposed. Additionally, this technique provides us a tool to express a particular structure as a function of associated aromatic, not aromatic and antiaromatic systems. From all the results here obtained we can conclude that consider the Carbó index as local instead of global, by the Hirschfeld partitioning, a relation between structures that differ only in one atom can be established. To obtain the polarization of heterocyclic systems as a function of the cyclopentadienyl molecule, we use the alignment method (TGSA) that also enables us to overcome the relative molecular orientation problem.

The descriptors proposed in this study also allow the description of new phenomena associated with local molecular orbital energies and molecular polarization in systems characterized by rigid structures and which only differ in one atom. Furthermore, as these methodologies are complementary, they enable us to relate some local physicochemical properties. The most important descriptor of the local similarity was the Coulomb index. It quantifies the differences between the dipole moments of the studied structures. Additionally, the method here proposed can contribute to the interpretation of chemical bonds, molecular interactions and molecular polarization under the action of an external electric field.

Hückel Method Proposed and Reactivity Descriptors on the DA Reactions

As the Hückel method is related with molecular topology (see Dewar-Zimmerman theory) in this research, a topological study on the DA reactions is conducted in order to quantify the global reactivity indexes using chemical reactivity and MQS. For the topological analysis we postulate that *"a system can be expressed in terms of another one".* This statement can be related to the intrinsic nature of conceptual DFT, here expressed as a function of local reactivity, obtaining results in good agreement with experimental data. In this topological analysis, we postulate new local reactivity indexes with the aim to quantify the chemical potential, hardness and electrophilicity. Furthermore, the chemical potential related with overlap and coulomb indexes reproduces the trend of the FF^- values associated with the C6 atom in the cycloaddition reaction, considering the C6 carbon atom as the responsible for the preferred stereochemistry, justifying the formation of the product P-24 in a polar stepwise process, and enabling the postulation of local reactivity indexes. This also represents an alternative for local indexes in the field of quantum similarity. In this regard, this dissertation contributes to gain new insights on the Hückel molecular orbital method using molecular polarization, quantum similarity and chemical reactivity in the DFT context.

References

1. M Mandado, C Van Alsenoy, P Geerlings, F De Proft, R A Mosquera, et al (2006) Hartree-Fock energy partitioning in terms of Hirshfeld atoms J Phys Chem 7(6): 1294-1305.
2. R Vivas Reyes, F De Proft, P Geerlings, M Biesemans, R Willem, et al. (2002) New J Chem 9: 1108.
3. F De Proft, R Vivas-Reyes, M Biesemans, R Willem, J M L Martin, et al. (2003) Eur J Inorg Chem 20: 3803.
4. R Vivas-Reyes, F De Proft, M Biesemans, R Willem, P Geerlings, et al. (2003) Eur J Inorg Chem 7: 1315.
5. I N Levine (1991) Quantum Chemistry Prentice Hall, Englewood Cliffs, New Jersey, USA.
6. R G Parr, D P Craig, I G Ross (1950) J Chem Phys 18: 1561.
7. R G Parr (1990) On the genesis of a theory. Int J Quant Chem 37: 327.
8. R B Woodward, R Hoffmann (1965) Orbital Symmetries and endo-exo Relationships in Concerted Cycloaddition Reactions. J Am Chem Soc 87: 395.
9. D A Bahnick (1994) Use of Huckel Molecular Orbital Theory in Interpreting the Visible Spectra of Polymethine Dyes: An Undergraduate Physical Chemistry Experiment. J Chem Edu 71: 171.
10. A Krishtal, P Senet, M Yang, C Van Alsenoy (2006) A Hirshfeld partitioning of polarizabilities of water clusters J Chem Phys 125(3): 34312.
11. A Krishtal, P Senet, C Van Alsenoy (2010) Origin of the size-dependence of the polarizability per atom in heterogeneous clusters: The case of AlP clusters. J Chem Phys 133(5): 154310.
12. A Morales Bayuelo, R Vivas Reyes (2012) Int J Mol Sci 24.
13. E Hückel (1931) Quantentheoretische Beiträge zum Benzolproblem. Zeitschrift für Physik 70: 204-286.
14. E Hückel (1932) Quantentheoretische Beiträge zum Problem der aromatischen und ungesättigten Verbindungen. Zeitschrift für Physik 76: 628-648.
15. C A Coulson, B O Leary, R B Mallion (1978) Hückel Theory for Organic Chemists.
16. A Streitwieser (1961) Molecular Orbital Theory for Organic Chemists.
17. P Bultinck, R Ponec, R Carbó Dorca (2007) Aromaticity in linear polyacenes: generalized population analysis and molecular quantum similarity approach. J Comput Chem 28: 152.
18. A Gallegos, D Robert, X Gironés, R Carbó Dorca (2001) Structure-toxicity relationships of polycyclic aromatic hydrocarbons using molecular quantum similarity. J Comput Aided Mol Des 15: 67-80.

19. R Carbó, M Arnau, L Leyda (1980) How similar is a molecule to another? An electron density measure of similarity between two molecular structures. Int J Quant Chem 17: 1185.
20. R Carbó Dorca, L D Mercado (2010) J Comput Chem 31: 2195.
21. X Gironés, R Carbó Dorca (2006) Modelling Toxicity using Molecular Quantum Similarity Measures. QSAR Comb Sci 25: 579.
22. R Carbó Dorca, E Besalú, L D Mercado (2011) J Comput Chem 32: 582.
23. R Carbó Dorca, X Gironés Int J Quant Chem 101: 8.
24. R Carbó Dorca, E Besalú (2010) Communications on quantum similarity (2): A geometric discussion on holographic electron density theorem and confined quantum similarity measures. J Comput Chem 31: 2452.
25. P G Mezey (1999) The holographic electron density theorem and quantum similarity measures. Mol Phys 96: 169.
26. A Morales Bayuelo, J Torres, R Vivas Reyes (2012) J Theor Comput Chem 11: 1.
27. C Kittel (1965) Introducción a la Física del estado sólido, Barcelona.
28. H Frólich (1958) Theory Dielectrics.
29. E W Mason (1964) Piezoelectric Crystals and their Application to Ultrasonics.
30. J C Anderson (1963) Dielectrics Chapman and Hall, London, UK.
31. A R vox (1954) Hippel Dielectric Materials and Applications New York, USA.
32. F Jona, G Shirane (1962) Ferroelectric Crystals. Wiley-VCH, London, UK.
33. K N Koen-Tanudzhi (1999) Uspekhi Fizicheskikh Nauk 169: 292.
34. C A Coulson, B O Leary, R B Mallion (1978) Hückel Theory for Organic Chemists.
35. A Streitwieser (1961) Molecular Orbital Theory for Organic Chemists, Wiley, New York, USA.
36. V Magnasco (2002) J Chem Phys 363: 544.
37. V Magnasco (2004) A Model for the Chemical Bond. J Chem Educ 81: 427.
38. V Magnasco (2003) J Chem Phys 380: 397. V Magnasco (2005) J Chem Phys 407: 213.
39. W Carruthers (1978) Some Modern Methods of Organic Synreview. Cambridge University Press, Cambridge, UK.
40. W Carruthers (1990) Cycloaddition Reactions in Organic Synreview.
41. Diels, K Alder (1928) Justus Liebigs Ann Chem 460: 98.
42. K Fukui (1964) Molecular Orbitals in Chemistry Physics and Biology, New York, USA.
43. H Eyring, MZ Polanyi (1931) Phys Chem Abt B 12: 279.
44. H Eyring (1935) Chem Rev 17: 65.
45. KJ Laidler, MC King (1983) Development of transition-state theory. J Phys Chem 87(15): 2657-2664.
46. DH Ess, GO Jones, KN Houk (2006) Conceptual, Qualitative, and Quantitative Theories of 1,3-Dipolar and Diels-Alder Cycloadditions Used in Synthesis. Adv Synth Catal 348(16-17): 2337-2361.
47. NYM Omar, NA Rahman, SM Zain (2011) Theoretical Insights into the Enantioselectivity and Mechanism of Diels-Alder Reactions Involving Chiral Cationic Oxazaborolidinium Catalyst. Bull Chem Soc 84(2): 196-204.
48. LR Domingo, MT Picher, P Arroyo (2006) A DFT study of the Huisgen 1,3-dipolar cycloaddition between hindered thiocarbonyl ylides and tetracyanoethylene. Tetrahedron 60(3): 5053-5058.
49. S Berski, J Andrés, B Silvi, LR Domingo (2006) New Findings on the Diels–Alder Reactions. An Analysis Based on the Bonding Evolution Theory. J Phys Chem A 110(51): 13939-13947.
50. A Morales Bayuelo (2013) Understanding the electronic reorganization in the thermal isomerization reaction of trans-3,4-dimethylcyclobutene. Origins of outward Pseudodiradical {2n + 2π} torquoselectivity. Inter J Quant Chem 113(10): 1534-1543.
51. LR Domingo, MJ Aurell, P Perez, R Contreras (2002) Quantitative characterization of the global electrophilicity power of common diene/dienophile pairs in Diels-Alder reactions. Tetrahedron 58(22): 4417-4423.
52. CH Chen, PD Rao, CC Liao (1998) Furans Act as Dienophiles in Facile Diels–Alder Reactions with Masked o-Benzoquinones. J Am Chem Soc 120(50): 13254-13255.
53. RG Parr, W Yang (1989) Density Functional Theory of Atoms and Molecules, Oxford University Press, New York, USA.
54. RG Parr, W Yang (1984) Density functional approach to the frontier-electron theory of chemical reactivity. J Am Chem Soc 106(14): 4049-4050.
55. a)E. Hückel (1931) Quanstentheoretische Beiträge zum Benzolproblem. Zeitschrift für Physik 72(5-6): 310-337.

    b)CA Coulson, B O'Leary, RB Mallion (1978) Hückel Theory for Organic Chemists. Academic Press, 1978.

    c)RB Woodward, R Hoffmann (1965) Stereochemistry of Electrocyclic Reactions. J Am Chem Soc 87(2): 395-397.

    d) Andrew Streitwieser (1961) Molecular Orbital Theory for Organic Chemists, Wiley, New York, USA.

    e) M Wolfsberg, LJ Helmholz (1952) The Spectra and Electronic Structure of the Tetrahedral Ions MnO_4^-, CrO_4^{--}, and ClO_4^-. J Chem Phys 20: 837.

    f) R. M. Tromer, JA Freire (2013) Extended Hückel Method Calculation of Polarization Energies: The Case of a Benzene Dimer. J Phys Chem A 117(51): 1427614281.
56. a) II Khvalchenko (2005) Polarization of Two Identical Atoms in an Electric Field. Russian Physics Journal 48(7): 729-732.

    b) E Wigner (1959) Group Theory and Its Application to the Quantum Mechanics of Atomic. Spectra, Academic Press. NY pp. 384.
57. a) P Bultinck, X Girones, R Carbó Dorca (2005) Reviews in Computational Chemistry 21: 127.

    b) P Bultinck, R Carbó Dorca (2004) Negative Fukui functions: New insights based on electronegativity equalization. J Math Chem 36: 191. B9
58. FL Hirschfeld (1977) heoretical chemistry accounts: Theory, computation and modeling. Theoretica Chimia Acta 44: 129.
59. X Girones, D Robert, R Carbó Dorca (2001) TGSA: A molecular superposition program based on topo-geometrical considerations. J Comp Chem 22(2): 255-263.
60. G Boon, C Van Alsenoy, F De Proft, P Bultinck, P Geerlings (2005) Molecular quantum similarity of enantiomers of amino acids: a case study. J Mol Struct: (THEOCHEM) 727(1-3): 49-56.
61. PG Mezey (1999) The holographic electron density theorem and quantum similarity measures. Mol Phys 96(2): 169-178.
62. A Morales Bayuelo, H Ayazo, Vivas Reyes (2010) Three-dimensional quantitative structure-activity relationship CoMSIA/CoMFA and LeapFrog studies on novel series of bicyclo [4.1.0] heptanes derivatives as melanin-concentrating hormone receptor R1 antagonists. R Eur J Med Chem 45(10): 4509-4522.
63. L Amat, R Carbó Dorca (1997) Quantum similarity measures under atomic shell approximation: First order density fitting using elementary Jacobi rotations. J Comput Chem 18(16): 2023-2039.

64. X Girones, D Robert, R Carbó Dorca (2001) TGSA: A molecular superposition program based on topo-geometrical considerations. J Comp Chem 22(2): 255-263.

65. P Constans, L Amat, R Carbó Dorca (1997) Toward a global maximization of the molecular similarity function: Superposition of two molecules. J Comp Chem 18(6): 826-846.

66. RF Nalewajski, RG Parr (2000) Information theory, atoms in molecules, and molecular similarity. Proceedings of the National Academy of Sciences of the United States of America 97(16): 8879-8882.

67. RG Parr, PW Ayers, RF Nalewajski (2005) What Is an Atom in a Molecule? J Phys Chem A 109(17): 3957-3959.

68. P Bultinck, T Kuppens, X Girones, R Carbó Dorca (2003) Quantum Similarity Superposition Algorithm (QSSA): A Consistent Scheme for Molecular Alignment and Molecular Similarity Based on Quantum Chemistry. J Chem Infor and Mod 43(4): 1143-1150.

69. PW Ayers (2006) Information Theory, the Shape Function, and the Hirshfeld Atom. Theor Chem Acc 115(5): 370-378.

70. PW Ayers (2000) J Chem Phys 113: 10886.

71. R K Roy, S Pal, K Hirao (1999) J Chem Phys 110: 8236.

72. P Bultinck, R Carbó Dorca, C Van Alsenoy (2003) Quality of Approximate Electron Densities and Internal Consistency of Molecular Alignment Algorithms in Molecular Quantum Similarity. J Chem Infor and Mod 43(4): 1208-1217.

73. L Amat, R Carbó Dorca (2002) Int J Quant Chem 87: 59.

74. P Constans, R Carbó Dorca (1995) J Chem Infor and Mod 35: 1046.

75. R Carbó Dorca, (2013) J Comp Chem 34: 766.

76. L Chen, P Bultinck, H De Winter, W Langenaeker (2003) Substructure and Maximal Common Substructure Searching. Tollenaere. (Edn.), Dekker, Inc, New York, USA, pp. 483.

77. MJ Frisch, GW Trucks, HB Schlegel, GE Scuseria, MA Robb, et al. (2015) Electronic Supplementary Material (ESI) for Chemical Science. GAUSSIAN 09, Revision A.02.

78. a) Roothaan CCJ(1951) New Developments in Molecular Orbital Theory. Rev Mod Phys 23: 69.

    b) People JA, Nesbet RK (1954) J Chem Phys 22: 571.

    c) Ma Weeny R, Dierksen G (1968) J Chem Phys 49: 4852.

    d)Becke AD (1993) J Chem Phys 98: 5648.

    e)Lee C, Yang W, Parr RG (1988) Development of the Colle-Salvetti correlation-energy formula into a functional of the electron density. Phys Rev B 37: 785.

    f) People JA, Beveridge DL (1970) Approximate Molecular Orbital Theory; McGraw Hill: New York, USA.

79. Parr RG, Yang WT (1984) Density functional approach to the frontier-electron theory of chemical reactivity. J Am Chem Soc 106: 4049.

80. Putz M (2006) Applications of Density Functional Theory to Biological and Bioinorganic. Int J Quant Chem 106: 361.

81. Bultinck P, Carbó-Dorca R (2004) J Math Chem 36: 191.

82. Parr RG, Yang W (1989) Density Functional Theory of Atoms and Molecules; Oxford University Press: New York,USA.

83. Bultinck P, Carbó-Dorca R (2005) Molecular quantum similarity using conceptual DFT descriptors. J Chem Sci 117: 425.

84. Hodgkin EE, Richards WG (1988) Chemical Reactivity Theory: A Density Functional View. Chem Ber Molecular Similarity 24: 1141.

85. Dreizler RM, Gross EKU (1990) Density functional theory. Springer, Berlin Heidelberg New York,USA.

86. Nalewajski RF, Parr RG(1982) Perspectives in Electronic Structure Theory.J Chem Phys 77: 399.

87. Randic M, Wilkins CL (1979) Handbook of Molecular Descriptors. J Chem Inf Comput Sci 19: 31.

88. Parr RG, Pearson RG (1983) Absolute hardness: companion parameter to absolute electronegativity. J Am Chem Soc 105: 7512-7516.

89. Berkowitz M, Parr RG (1988) J Chem Phys 88: 2554.

90. Weisstein EW (2003) Encyclopedia of Mathematics, Chapman & Hall, London,UK.

91. Rouvray DH (1995) Topics in Current Chemistry173:1.

92. Haskopoulos A, Maroulis G (2010) Chem Phy 367:127.

93. Krishtal A, Senet P, Yang M, Van Alsenoy C (2006) J Chem Phy 125: 034312.

94. Krishtal A, Senet P, Van C Alsenoy (2010) Origin of the size-dependence of the polarizability per atom in heterogeneous clusters: the case of AlP clusters. J Chem Phy 133: 154310.

95. Morales-Bayuelo A, Torres J, Vivas-Reyes RJ (2012) Theo and Comp Chem 11:1.

96. Morales-Bayuelo R, Vivas-Reyes (2012) Theoretical Model for the Molecular Polarization of Thiophene under the Action of an-Electric Field Using Topo-Geometrical Superposition Algorithm (TGSA) Int J Mol Sci.

97. Tomasi J, Mennucci B, Cammi R (2005) Chem Rev 105 :2999.

98. Mennucci J, Tomasi (2002) Polarizable Continuum Model (PCM) Calculations of Solvent Effects on Optical Rotations of Chiral Molecules. J Phys Chem A 106: 6102.

99. Parr RG (1984) Remarks on the concept of an atom in a molecule and on charge transfer between atoms on molecule formation. Int J Quant Chem 26: 687-692.

100. Bally T, Chai S, Neuenschwander M, Zhu Z (1869) CRC Handbook of Organic Photochemistry and Photobiology, Volumes 1 & 2. J Am Chem Soc 119.

101. Cotton FA (1990) Chemical Applications of group theory, 3rd (Edn.). A Wiley-Interscience publication 152.

102. Rouvray DH(1992) J Chem Inf Comput Sei 32: 580.

103. Morales-Bayuelo A, Ayazo A, Vivas-Reyes H (2010) R Eur J Med Chem 10: 4509.

104. Girones X, Robert D, Carbó-Dorca R (2001) Chemical Reactivity Theory: A Density Functional View. J Comp Chem 22: 255.

105. Bader R (1990) Atoms in Molecules: A Quantum Theory; Oxford University Press: Oxford,UK.

106. Chattaraj PK, Cedillo A, Parr RG (1995) Concepts and Methods in Modern Theoretical Chemistry: Electronic Structure. J Chem Phys 103:10621.

107. Ayers PW, Levy M (2000) Theor Chem Acc 103: 353.

108. Domingo LR, Aurell MJ (2002) J Org Chem 67: 959.

ISSN: 2574-1241

DOI: 10.26717/BJSTR.2020.25.004187

Alejandro Morales Bayuelo. Biomed J Sci & Tech Res